UNIVERSITÀ DEGLI STUDI DI PAVIA
FACOLTÀ DI INGEGNERIA
Dipartimento di Meccanica Strutturale

HOMOGENEOUS AND MULTILAYERED BEAM MODELS: VARIATIONAL DERIVATION, ANALYTICAL AND NUMERICAL SOLUTIONS

Modelli di Travi Omogenee e Multistrato: Derivazione Variazionale, Risultati Analitici e Numerici

Supervisor: Professor
FERDINANDO AURICCHIO

Co - supervisors: Professors
CARLO LOVADINA
GIANCARLO SANGALLI

Author:
GIUSEPPE BALDUZZI

Academic year 2006/2007

Ringraziamenti

Lo svolgimento di questo lavoro e soprattutto il raggiungimento di questo traguardo non sarebbe stato possibile senza il contributo di molte persone che mi hanno aiutato, consigliato, pazientemente sopportato.

Il primo ringraziamento va al prof. Auricchio per l'infinita disponibilità e la sollecitudine che ha sempre avuto nel seguirmi nello svolgimento di questo lavoro. Ringrazio poi i correlatori , il prof. Lovadina e il prof. Sangalli, per la loro pazienza nello spiegarmi come risolvere i problemi che ho incontrato nel mio lavoro.
Non posso poi dimenticare Alessandro Reali, Michele Conti e tutto il gruppo di ricerca del professore: non mi hanno mai fatto mancare il loro sostegno morale e pratico nei passaggi più difficili. In ultimo voglio ringraziare la professoressa Chiara Plebani e Giovanni Borghese per avermi aiutato nella redazione dei testi in lungua inglese.

Un grazie speciale a mio padre che mi ha insegnato ad osservare e stupirsi del mondo e a mia madre che senza una parola mi ha spiegato cosa sia la perseveranza: per avermi sempre sostenuto in questi anni e l'enorme fiducia che hanno avuto nei miei confronti. So che anche per loro non è sempre stato facile fare o lasciarmi fare certe scelte.
Ringrazio poi le mie sorelle Patrizia e Luigina per la loro vicinanza, le mani sempre tese per ogni problema e, last but not least, per la macchina.
Ringrazio i miei nipoti Andrea e Stefano anche se in realtà dovrebbero essere loro a ringraziare me per la gentile sopportazione ...
Un grazie a tutti i parenti che, sempre ed in ogni modo, non mi hanno mai fatto mancare il loro sotegno e il loro aiuto.
Ringrazio tutti gli amici, quelli di su e quelli di giù, quelli del collegio e quelli di via Tavazzani, quelli dell'università e quelli delle superiori. In avventure e disavventure, in piaceri e dispiaceri mai sono rimasto solo. Se chi trova un amico trova un tesoro probabilmente sono una delle persone più ricche del pianeta.
Ringrazio infine tutti miei professori, maestri, insegnanti: non potrei essere qua se non fossi stato guidato da persone valide.

Abstract

The purpose of this work is to operate a *dimensional reduction* from the 3D problem to a 1D problem. This operation leads to a so-called beam model. The procedure permits to reduce the complexity of the problem but at the same time it introduces some approximations. The model goodness can be seen as the best compromise between approximation and accuracy.

In this thesis we will discuss some models of plane beam. The material is linear, elastic and isotropic. We will consider first an homogeneous section and after a laminated beam, made by layers of different materials. The first purpose of our work is to obtain a model that could predict the behavior of the beam in exact way, without the need to introduce any correction factor, as it appened for the Timoshenko model.

To develop the beam model we will use the stationarity conditions of functionals. Specifically we will use the virtual work principle, the Hellinger-Reissner functional and the Hu Washitzu functional. Each of these has good and bad properties. In the next chapters we will use them to highlight the significant merits and failings.

Starting from the homogeneous beam we will try to generalize the model to a laminated beam for which we will develop the governing equation and find some analytical solutions to discuss the model goodness. For the latter, we will build also a numerical model, write the algebraic equations and find some numerical solutions.

Riassunto

Lo scopo di questa tesi è operare una *riduzione diemensionale*: partendo da una formulazione in 3D vogliamo arrivare ad un problema monodimensionale. Questa operazione porta ai cosiddetti modelli di trave. La procedura permette di ridurre la complessità del problema ma al tempo stesso introduce alcune approssimazioni. La bontà dei modelli così ottenuti può essere vista come il miglior compromesso fra il grado di approssimazione e l'accuratezza degli stessi.

In questa tesi ci occuperemo di alcuni modelli di trave piana. Assumiamo che il materiale sia lineare, elastico ed isotropo. In prima istanza considereremo una trave omogenea, successivamente generalizzeremo il modello ad una trave laminata, ovvero costituita da strati orizzontali di materiali diversi. Il primo obiettivo del nostro lavoro sarà quello di ottenere un modello che possa predire correttamente il comportamento della trave, in particolare senza l'introduzione di alcun fattore di correzzione come invece succede nella trave di Tomoshenko.

Per ricavare le equazioni della trave useremo, oltre ai classici metodi variazionali, la stazionarietà di alcuni funzionali. In particolare faremo uso del principio dei lavori virtuali, del funzionale di Hellinger-Reissner e di quello di Hu Washitzu; ognuno di essi presenta, nel suo impiego, limiti e svantaggi: nella derivazione delle equazioni ci proponiamo anche di mettere in luce i punti di forza ed i difetti di ogni metodo che useremo.

Partendo dalla trave omogenea cercheremo di generalizzare il modello ad una trave laminata per la quale scriveremo le equazioni governanti. Cercheremo anche di ricavare alcune soluzioni analitiche per constatarne la bontà. Per la trave laminata svilupperemo infine un modello numerico per il quale vogliamo ricavare le equazioni algebriche che lo governano e, utilizzando queste ultime, cercare alcune soluzioni per casi elementari al fine di discuterne l'efficacia.

Contents

Chapter 1

Introduction

This chapter starts with a brief review of the state of the art about the subject of the present thesis followed by the definition of the problem we study, the introduction of our hypotheses and the tools we are going to use for our developments.

1.1 State of the art

The majority of structural members can be efficiently modeled by one-dimensional elements, just this statement may justify the high interest of civil engineering researchers on this topic.
In the past, when calculators were not available, engineers developed beam models to reduce as much as possible the unknowns of the problem they were analyzing. A class of models created for this purpose is the so called first-order, plane, kinematics beams.
The Euler-Bernoulli beam can be considered the most significant example of this class, by means of it the 3D, homogeneous, elastic problem is reduced to a simple ODE (Ordinary Differential Equation) system in 2 one-dimensional uncoupled unknows. Even today, when more accurate models and more powerful instruments are available, this model is the most used. Its simplicity allows to obtain the solution by direct integration of transversal load, as illustrated in [10].
The other most significant first-order model is the Timoshenko beam where axial, transversal displacements and section rotation are the unknown one-dimensional fields. Timoshenko beam allows uncoupling the axial and the shear-bending problems.
Obviously these models show some important limitations: the solutions correspond to the real behavior of the body only if the ratio between length and transversal dimension is $\gg 1$, the models predict only the stress resultant so local effects of force distribution or kinematic constrains can not be con-

sidered. Additionally every model has got specific limitations, as example the Timoshenko beam needs to be correct by shear factor and its solution is valid if length-thickness ratio ≥ 4, the Euler-Bernoulli solution is valid when length-thickness ratio ≥ 10.

The necessity of most accurate models and the numerical methods nowadays available induce researchers to develop the so called high-order beam models. They are developed starting from a complicated section kinematics, usually described by high order polynomials.
Limiting our interest to plane beams, the most famous high-order model is the Reddy beam that considers the shear section warping, on the opposite, the most complete model is the Lo-Christenson-Wu beam where authors consider the most complete kinematics. For a general treatment of high-order plane kinematic beam models see [14].

Often the use of more accurate models is justified by the necessity to describe the behavior of advanced materials or elements as laminated or multi-layered beams and plates, orthotropic or inelastic bodies .... Multi-layered beams are obtained by union of different material layers. The purpose is to obtain a structural element in which every component exalts its specific properties and the global answer is better than the single component behavior. The applications of these structures are many and they span from civil to mechanical, naval and aerospace engineering.
Literature around laminated beam and plate modeling is very rich, there exist analytical and exact models (see [11] and [12]) but also numerical methods are developed (as example see [16]).
Usually these models try to describe the displacement field by section globally defined functions, so it is possible to predict only global displacements and medium stresses. On contrary in this work we try to develop a model in which displacement and stress fields are locally defined so that it is possible to evaluate more accurately the real stresses inside the body.

1.2 Domain and field definitions

In this section we use notation adopted in [1].
Let A be a closed domain in $\mathbb{R}^2$, $[0,l]$ a closed interval in $\mathbb{R}$. We call A section and l longitudinal axis. We define them rigorously as follows:

$$A = \left\{ (y,z) \in \mathbb{R}^2 \quad | \quad y \in [-\frac{h}{2}, \frac{h}{2}], z \in [-\frac{b}{2}, \frac{b}{2}] \right\} \tag{1.1}$$

Let Ω be the solid occupying the region:

$$\Omega = A \times [0,l] \tag{1.2}$$

and let we call it beam.
Obviously $l \gg h \approx b$ so that it is possible to recognize a predominant dimension. The domain scheme and the Cartesian coordinate system we adopt are represented in figure 1.1.

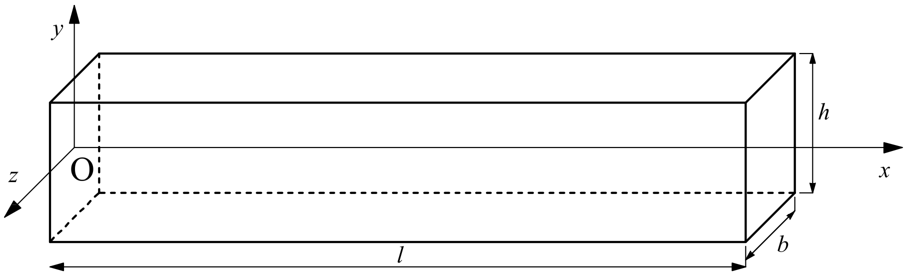

Figure 1.1: Coordinate system and geometry of the solid we are studying

We define $A_{0,l} = A \times \{0, l\}$ extreme sections of the beam and we call $S_{\pm\frac{h}{2}} = (0, l) \times \{\pm\frac{h}{2}\} \times (-\frac{b}{2}, \frac{b}{2})$ and $S_{\pm\frac{b}{2}} = (0, l) \times (-\frac{h}{2}, \frac{h}{2}) \times \{\pm\frac{b}{2}\}$ lateral surfaces of the solid. We denote $\partial\Omega = A_{0,l} \cup S_{\pm\frac{h}{2}} \cup S_{\pm\frac{b}{2}}$ as boundary of domain.
Consider $\{\partial\Omega_t; \partial\Omega_s\}$, a partition of $\partial\Omega$. Let $\partial\Omega_t$ and $\partial\Omega_s$ be respectively the force boundary and the displacement constrained surfaces.
Let Ω be a plane beam hence we do not consider forces in z direction. Additionally we make hypothesis of plane stress state, this means that stresses in z direction are null (i.e. $\sigma_{zz} = \tau_{xz} = \tau_{yz} = 0$). These two hypotheses lead to consider z direction deformations and displacements as dependent or trivial variables. For all these reasons $S_{\pm\frac{b}{2}}$ became a not significant domain boundary so we will not consider it in the following developments.
We suppose that the beam is loaded by a surface force density $\boldsymbol{t} : \partial\Omega_t \to \mathbb{R}^2$ and a volume force density $\boldsymbol{f} : \Omega \to \mathbb{R}^2$, moreover on $\partial\Omega_s$ we define the boundary displacement function: $\bar{\boldsymbol{s}} : \partial\Omega_s \to \mathbb{R}^2$.
The beam is made by isotropic, linear, elastic material. For the final work purpose we do not consider homogeneity hypothesis. To define the mechanical properties in the body we must introduce the scalar fields $E : A \to \mathbb{R}$ and $G : A \to \mathbb{R}$, obviously they can not be completely independent each other in fact E and G are linked by ν that $\in \left[0\,,\frac{1}{2}\right[$.

Considering the plane beam hypothesis we must define the following independent variable fields:

$$\boldsymbol{\sigma} : \Omega \rightarrow \mathbb{R}^{2\times 2} \tag{1.3a}$$
$$\boldsymbol{\varepsilon} : \Omega \rightarrow \mathbb{R}^{2\times 2} \tag{1.3b}$$
$$\boldsymbol{s} : \Omega \rightarrow \mathbb{R}^{2} \tag{1.3c}$$

in which stress $\boldsymbol{\sigma}$ and strain $\boldsymbol{\varepsilon}$ are symmetric tensors and displacements $\boldsymbol{s}$ is a vectorial field.

1.3 3D problem definition

The elastic solid problem may be formulated in many ways, nevertheless we can classify all the formulations as derived by two paths.

- **Strong formulation** that is the most intuitive path, it consists in requiring that displacements, stresses and strains satisfy in each point inside the domain compatibility, equilibrium and constitutive relations. This formulation brings to an PDE (Partial Differential Equations) system.
- **Weak formulation** that is the most useful for some aspects, it consists in requiring stationarity of a scalar quantity. This path brings to write an integro-differential equation. Energy methods belong to this class of formulations.

For many aspects the two paths are equivalent and they give the same solution. Watching at the context and the work purpose, we may choose the formulation that better satisfy our needs.

1.3.1 Strong formulation

On the domain we want to satisfy the boundary value problem:

$$\boldsymbol{\varepsilon} = \nabla^{s}\boldsymbol{s} \tag{1.4a}$$
$$\boldsymbol{\sigma} = \boldsymbol{D} : \boldsymbol{\varepsilon} \qquad \text{in}\ \Omega \tag{1.4b}$$
$$\nabla \cdot \boldsymbol{\sigma} + \boldsymbol{f} = \boldsymbol{0} \tag{1.4c}$$
$$\boldsymbol{\sigma} \cdot \boldsymbol{n} = \boldsymbol{t} \qquad \text{in}\ \partial\Omega_t \tag{1.4d}$$
$$\boldsymbol{s} = \bar{\boldsymbol{s}} \qquad \text{in}\ \partial\Omega_s \tag{1.4e}$$

in which $\boldsymbol{D}$ is the fourth order tensor of the constitutive relations.
Equation (1.4a) is the compatibility relation, valid for small displacements and small displacement gradients, equation (1.4b) is the material constitutive relation and equation (1.4c) represents the equilibrium condition. Equations (1.4d) and (1.4e) are respectively the boundary equilibrium and the boundary compatibility conditions.

1.3.2 Total Potential Energy and Virtual Work Principle approach

The functionals we are introducing is the most used in continuum mechanics: in basic literature (as [7] and [8]) the first-order beams are developed starting from these principles.

VWP can be written as:

$$\delta W_{VWP} = \int_{\Omega} \delta\boldsymbol{\varepsilon} : \boldsymbol{\sigma}\, d\Omega - \int_{\Omega} \delta\boldsymbol{s} \cdot \boldsymbol{f}\, d\Omega - \int_{\partial\Omega_t} \delta\boldsymbol{s} \cdot \boldsymbol{t}\, dS = 0 \tag{1.5}$$

in which deformation $\boldsymbol{\varepsilon}$ is compatible (i.e. it satisfies equation (1.4a)) and stress $\boldsymbol{\sigma}$ is equilibrate (i.e. it satisfies equation (1.4c)).
It is remarkable that this principle can be applied to every body independently by constitutive relation (1.4b).

TPE functional can be used only for an elastic body, for which fields are conservative and it is formulated as follows:

$$J_{TPE}(\boldsymbol{s}) = \frac{1}{2}\int_{\Omega} \nabla^s \boldsymbol{s} : \boldsymbol{D} : \nabla^s \boldsymbol{s}\, d\Omega - \int_{\Omega} \boldsymbol{s} \cdot \boldsymbol{f}\, d\Omega - \int_{\partial\Omega_t} \boldsymbol{s} \cdot \boldsymbol{t}\, dS \tag{1.6}$$

Its stationarity can be expressed as:

$$\delta J_{TPE}(\boldsymbol{s}) = \int_{\Omega} \nabla^s (\delta\boldsymbol{s}) : \boldsymbol{D} : \nabla^s \boldsymbol{s}\, d\Omega - \int_{\Omega} \delta\boldsymbol{s} \cdot \boldsymbol{f}\, d\Omega - \int_{\partial\Omega_t} \delta\boldsymbol{s} \cdot \boldsymbol{t}\, dS = 0 \tag{1.7}$$

For an elastic body, expressing $\boldsymbol{\sigma}$ and $\boldsymbol{\varepsilon}$ as function of $\boldsymbol{s}$, VWP and TPE stationarity give the same equation. In the following, since we are going to consider only elastic bodies, we could use the 2 approach indifferently but for more simplicity we will speak of VWP.

Expressing all terms as function of $\boldsymbol{s}$ the first term of equation (1.5) could be written as follows:

$$\int_{\Omega} \nabla^s (\delta\boldsymbol{s}) : \boldsymbol{D} : \nabla^s \boldsymbol{s}\, d\Omega = \int_{\partial\Omega} \delta\boldsymbol{s} \cdot (\boldsymbol{D} : \nabla^s \boldsymbol{s}) \cdot \boldsymbol{n}\, dS - \int_{\Omega} \delta\boldsymbol{s} \cdot \nabla \cdot (\boldsymbol{D} : \nabla^s \boldsymbol{s})\, d\Omega \tag{1.8}$$

Subdividing the integral defined on the surface in the integrals on $\partial\Omega_t$ and on $\partial\Omega_s$, equation (1.7) can be rewritten as:

$$\begin{aligned}\delta W_{VWP}(\boldsymbol{s}) = &-\int_{\Omega} \delta\boldsymbol{s} \cdot (\nabla \cdot (\boldsymbol{D} : \nabla^s \boldsymbol{s}) + \boldsymbol{f})\, d\Omega + \\ &\int_{\partial\Omega_t} \delta\boldsymbol{s} \cdot ((\boldsymbol{D} : \nabla^s \boldsymbol{s}) \cdot \boldsymbol{n} - \boldsymbol{t})\, dS + \int_{\partial\Omega_u} \delta\boldsymbol{s} \cdot (\boldsymbol{D} : \nabla^s \boldsymbol{s}) \cdot \boldsymbol{n} = 0\end{aligned} \tag{1.9}$$

It is possible to see that the first term contains the equilibrium relation expressed as function of displacements. The second term contains the force boundary conditions. Since it is defined on the displacement constrained boundary, considering on it a non-null virtual displacement the last term give the constrain reactions but, having these quantities low interest in this work, we will consider the virtual displacements always null and this term will be omit.

It is important to see that in VWP boundary compatibility conditions do not appear, we could expect this because the principle give only the equilibrium condition.
An alternative VWP formulation to (1.7) from which we can start is:

$$\delta J_{TPE}(\boldsymbol{s}) = -\int_\Omega \delta\boldsymbol{s}\cdot(\nabla\cdot(\boldsymbol{D}:\nabla^s\boldsymbol{s}) + \boldsymbol{f})\, d\Omega + \int_{\partial\Omega_t} \delta\boldsymbol{s}\cdot((\boldsymbol{D}:\nabla^s\boldsymbol{s})\cdot\boldsymbol{n} - \boldsymbol{t})\ dS = 0 \tag{1.10}$$

1.3.3 Hellinger-Reissner approach

The Hellinger-Reissner functional (shortly HR) can be expressed as follows:

$$\begin{aligned} J_{HR}(\boldsymbol{\sigma},\boldsymbol{s}) = &\int_\Omega \boldsymbol{\sigma}:\nabla^s\boldsymbol{s}\, d\Omega - \frac{1}{2}\int_\Omega \boldsymbol{\sigma}:\boldsymbol{D}^{-1}:\boldsymbol{\sigma}\, d\Omega - \int_\Omega \boldsymbol{s}\cdot\boldsymbol{f}\, d\Omega \\ &- \int_{\partial\Omega_t} \boldsymbol{s}\cdot\boldsymbol{t}\, dS - \int_{\partial\Omega_s} \boldsymbol{\sigma}\cdot\boldsymbol{n}\cdot(\boldsymbol{s}-\bar{\boldsymbol{s}})\ dS \end{aligned} \tag{1.11}$$

Its stationarity condition is:

$$\begin{aligned} \delta J_{HR} = &\int_\Omega \nabla^s\delta\boldsymbol{s}:\boldsymbol{\sigma}\, d\Omega + \int_\Omega \delta\boldsymbol{\sigma}:\nabla^s\boldsymbol{s}\, d\Omega - \\ &\int_\Omega \delta\boldsymbol{\sigma}:\boldsymbol{D}^{-1}:\boldsymbol{\sigma}\, d\Omega - \int_\Omega \delta\boldsymbol{s}\cdot\boldsymbol{f}\, d\Omega - \int_{\partial\Omega_t} \delta\boldsymbol{s}\cdot\boldsymbol{t}\, dS - \\ &\int_{\partial\Omega_s} \delta\boldsymbol{\sigma}\cdot\boldsymbol{n}\cdot(\boldsymbol{s}-\bar{\boldsymbol{s}})\ dS - \int_{\partial\Omega_s} \delta\boldsymbol{s}\cdot\boldsymbol{\sigma}\cdot\boldsymbol{n}\, dS = 0 \end{aligned} \tag{1.12}$$

The first term of (1.12) could be expressed as:

$$\int_\Omega \nabla^s\delta\boldsymbol{s}:\boldsymbol{\sigma}\, d\Omega = \int_{\partial\Omega} \delta\boldsymbol{s}\cdot\boldsymbol{\sigma}\cdot\boldsymbol{n}\, dS - \int_\Omega \delta\boldsymbol{s}\cdot\nabla\cdot\boldsymbol{\sigma}\, d\Omega \tag{1.13}$$

Substituting equation (1.13) in (1.12) and collecting the terms that use the same virtual degrees of freedom we obtain:

$$\delta J_{HR} = \int_\Omega \delta\boldsymbol{\sigma} : \left(\nabla^s \boldsymbol{s} - \boldsymbol{D}^{-1} : \boldsymbol{\sigma}\right) \, d\Omega - \tag{1.14a}$$

$$\int_\Omega \delta\boldsymbol{s} \cdot (\nabla \cdot \boldsymbol{\sigma} + \boldsymbol{f}) \, d\Omega + \tag{1.14b}$$

$$\int_{\partial\Omega_t} \delta\boldsymbol{s} \cdot (\boldsymbol{\sigma} \cdot \boldsymbol{n} - \boldsymbol{t}) \, dS - \tag{1.14c}$$

$$\int_{\partial\Omega_s} \delta\boldsymbol{\sigma} \cdot \boldsymbol{n} \cdot (\boldsymbol{s} - \bar{\boldsymbol{s}}) \, dS = 0 \tag{1.14d}$$

It is possible to see that term (1.14a) contains constitutive and compatibility relations. Term (1.14b) is the weak expression of equilibrium relation inside the body meanwhile (1.14c) is the force boundary equilibrium, term (1.14d) is the displacement constrained surface compatibility.

1.3.4 Hu-Washizu approach

The Hu-Washizu functional (shortly HW) may be expressed as follows:

$$\begin{aligned} J_{HW}(\boldsymbol{\sigma}, \boldsymbol{\varepsilon}, \boldsymbol{s}) = &\int_\Omega \boldsymbol{\sigma} : (\nabla^s \boldsymbol{s} - \boldsymbol{\varepsilon}) \, d\Omega + \frac{1}{2} \int_\Omega \boldsymbol{\varepsilon} : \boldsymbol{D} : \boldsymbol{\varepsilon} \, d\Omega - \int_\Omega \boldsymbol{s} \cdot \boldsymbol{f} \, d\Omega \\ &- \int_{\partial\Omega_t} \boldsymbol{s} \cdot \boldsymbol{t} \, dS - \int_{\partial\Omega_s} \boldsymbol{\sigma} \cdot \boldsymbol{n} \cdot (\boldsymbol{s} - \bar{\boldsymbol{s}}) \, dS \end{aligned} \tag{1.15}$$

Its stationarity condition can be expressed as:

$$\begin{aligned} \delta J_{HW} = &\int_\Omega \nabla^s \delta\boldsymbol{s} : \boldsymbol{\sigma} \, d\Omega - \int_\Omega \delta\boldsymbol{\varepsilon} : \boldsymbol{\sigma} \, d\Omega + \int_\Omega \delta\boldsymbol{\sigma} : (\nabla^s \boldsymbol{\sigma} - \boldsymbol{\varepsilon}) \, d\Omega + \\ &\int_\Omega \delta\boldsymbol{\varepsilon} : \boldsymbol{D} : \boldsymbol{\varepsilon} \, d\Omega - \int_\Omega \delta\boldsymbol{s} \cdot \boldsymbol{f} \, d\Omega - \int_{\partial\Omega_t} \delta\boldsymbol{s} \cdot \boldsymbol{t} \, dS - \\ &\int_{\partial\Omega_s} \delta\boldsymbol{\sigma} \cdot \boldsymbol{n} \cdot (\boldsymbol{s} - \bar{\boldsymbol{s}}) \, dS - \int_{\partial\Omega_s} \delta\boldsymbol{s} \cdot \boldsymbol{\sigma} \cdot \boldsymbol{n} \, dS = 0 \end{aligned} \tag{1.16}$$

The first term of (1.16) can be expressed as follows (this expression is the same of (1.13)):

$$\int_\Omega \nabla^s \delta\boldsymbol{s} : \boldsymbol{\sigma} \, d\Omega = \int_{\partial\Omega} \delta\boldsymbol{s} \cdot \boldsymbol{\sigma} \cdot \boldsymbol{n} \, dS - \int_\Omega \delta\boldsymbol{s} \cdot \nabla \cdot \boldsymbol{\sigma} \, d\Omega \tag{1.17}$$

Substituting equation (1.17) in (1.16) and collecting terms that use the same virtual degrees of freedom we obtain:

$$\delta J_{HW} = \int_{\Omega} \delta\boldsymbol{\sigma} : (\nabla^s \boldsymbol{s} - \boldsymbol{\varepsilon})\ d\Omega + \tag{1.18a}$$

$$\int_{\Omega} \delta\boldsymbol{\varepsilon} : (\boldsymbol{D} : \boldsymbol{\varepsilon} - \boldsymbol{\sigma})\ d\Omega - \tag{1.18b}$$

$$\int_{\Omega} \delta\boldsymbol{s} \cdot (\nabla \cdot \boldsymbol{\sigma} + \boldsymbol{f})\ d\Omega + \tag{1.18c}$$

$$\int_{\partial\Omega_t} \delta\boldsymbol{s} \cdot (\boldsymbol{\sigma} \cdot \boldsymbol{n} - \boldsymbol{t})\ dS - \tag{1.18d}$$

$$\int_{\partial\Omega_s} \delta\boldsymbol{\sigma} \cdot \boldsymbol{n} \cdot (\boldsymbol{s} - \bar{\boldsymbol{s}})\ dS = 0 \tag{1.18e}$$

As happened in section 1.3.3 we can recognize that HW stationarity condition corresponds to a weak imposition of the 3D elastic solid governing equations ((1.4)): term (1.18a) contains compatibility relation (1.4a), term (1.18b) contains constitutive relation (1.4b), term (1.18c) contains equilibrium (1.4c), (1.18d) and (1.18e) respectively require boundary equilibrium (1.4d) and boundary compatibility(1.4e).

1.3.5 Conclusions on problem formulations

At the end of this chapter we can make some remarks on the problem formulations we have just presented.

- Every weak approach can be expressed by two formulations: the former derives directly by functional stationarity, the latter can be seen, more easily, as weighted imposition of strong formulation. The former leads to a symmetric formulation, while the latter leads to an un-symmetric one. The choice of the formulation from which to start produce enormously different models.

- To be applied, TPE functional needs the stronger hypotheses but it is also the most elementary principle, on the opposite we can use HW more freely even if it is the most complicate approach. The trade-off between the problem complexity and the wanted approximation is the most common criterion to choose the formulation we must use to develop the model.

Chapter 2

Homogeneous beam models

In this chapter, starting from the weak formulations presented in section 1.3, we develop some homogeneous beam models. The idea that leads to derive the model is the so called "*dimensional reduction*" of the 2D problem[1] we previously defined that consists in reducing to a finite dimension the number of degrees of freedom that fields have respect to the section variables.
To this purpose we start defining more clearly the finite dimension field hypotheses and introducing efficient notation, then we derive some significant first- and high-order beams and finally we make some numerical example to illustrate differences between models, faults, limitations, good behaviors.

2.1 Hypotheses

2.1.1 Fields definition

We impose that every component $\alpha(x, y)$ of field $\boldsymbol{A}$ may be expressed as scalar product of vector $\boldsymbol{p_\alpha} : [-\frac{h}{2}, \frac{h}{2}] \to \mathbb{R}$ (called section base field vector) with vector $\boldsymbol{\alpha} : l \to \mathbb{R}$ (called section magnitude field vector). Choosing a finite dimension for $\boldsymbol{p_\alpha}$, we constrain the shape of field but at the same time we eliminate one order of infinitive.
This hypothesis is very strong in fact it leads to express fields simply as properties of the section, obviously the choice of $\boldsymbol{p_\alpha}$ components must be carefully because model accuracy and effectiveness depend on it.
Moreover it is remarkable that with this assumption field partial derivatives can be written as total differential of basis functions or of magnitude func-

[1]This expression is used in [1]. We adopt it because it express clearly what we are going to do.

tions, as displayed in the following.

$$\begin{aligned} \frac{\partial}{\partial y}\alpha(x,y) &= \frac{\partial}{\partial y}\left(\boldsymbol{p_\alpha}^T(y)\,\boldsymbol{\alpha}(x)\right) = \frac{d}{dy}\boldsymbol{p_\alpha}^T(y)\,\boldsymbol{\alpha}(x) = \boldsymbol{p_\alpha}'^T\,\boldsymbol{\alpha} \\ \frac{\partial}{\partial x}\alpha(x,y) &= \frac{\partial}{\partial x}\left(\boldsymbol{p_\alpha}^T(y)\boldsymbol{\alpha}(x)\right) = \boldsymbol{p_\alpha}^T(y)\,\frac{d}{dx}\boldsymbol{\alpha}(x) = \boldsymbol{p_\alpha}^T\,\boldsymbol{\alpha}' \end{aligned} \tag{2.1}$$

In this work we will never consider σ_{yy} and ε_{yy} because they are not considered significant variables in the problem, in other words we are going to consider alwais a constant transversal displacement on the section. To operate more easily on tensor fields we express them, formally, as vectors. Adopting also the previous approximations, unknown fields can be expressed as follows:

$$\boldsymbol{s}\left\{\begin{array}{c} s_u \\ s_v \end{array}\right\} = \left\{\begin{array}{c} \boldsymbol{p_u}^T\,\boldsymbol{u} \\ \boldsymbol{p_v}^T\,\boldsymbol{v} \end{array}\right\} \tag{2.2a}$$

$$\boldsymbol{\sigma} \Rightarrow \left\{\begin{array}{c} \sigma_{xx} \\ \tau_{xy} \end{array}\right\} = \left\{\begin{array}{c} \boldsymbol{p_\sigma}^T\,\boldsymbol{\sigma_x} \\ \boldsymbol{p_\tau}^T\,\boldsymbol{\tau} \end{array}\right\} \tag{2.2b}$$

$$\boldsymbol{\varepsilon} \Rightarrow \left\{\begin{array}{c} \varepsilon_{xx} \\ \gamma_{xy} \end{array}\right\} = \left\{\begin{array}{c} \boldsymbol{p_\varepsilon}^T\,\boldsymbol{\varepsilon_x} \\ \boldsymbol{p_\gamma}^T\,\boldsymbol{\gamma} \end{array}\right\} \tag{2.2c}$$

$$\tag{2.2d}$$

in which $\gamma = 2\varepsilon_{xy}$. Virtual fields $\delta\boldsymbol{A}$ use the same base field vectors of the correspondent real one.

2.1.2 Operators

In coherence with the notation just introduced, we must re-define the differential operators, the normal versor product and the matrix that appear in the problem formulations.

$$\nabla\cdot\boldsymbol{\sigma} \Rightarrow \qquad \boldsymbol{L\sigma} = \left(\frac{\partial}{\partial x}\boldsymbol{E_1} + \frac{\partial}{\partial y}\boldsymbol{E_2}\right)\left\{\begin{array}{c} \boldsymbol{p_\sigma}^T\boldsymbol{\sigma_x} \\ \boldsymbol{p_\tau}^T\,\boldsymbol{\tau} \end{array}\right\} \tag{2.3a}$$

$$\nabla^s\boldsymbol{s} \Rightarrow \qquad \boldsymbol{L}^T\boldsymbol{s} = \left(\frac{\partial}{\partial x}\boldsymbol{E_1} + \frac{\partial}{\partial y}\boldsymbol{E_2}^T\right)\left\{\begin{array}{c} \boldsymbol{p_u}^T\,\boldsymbol{u} \\ \boldsymbol{p_v}^T\,\boldsymbol{v} \end{array}\right\} \tag{2.3b}$$

$$\boldsymbol{\sigma}\cdot\boldsymbol{n} \Rightarrow \qquad \boldsymbol{N\sigma} = (n_x\boldsymbol{E_1} + n_y\boldsymbol{E_2})\left\{\begin{array}{c} \boldsymbol{p_\sigma}^T\boldsymbol{\sigma_x} \\ \boldsymbol{p_\tau}^T\,\boldsymbol{\tau} \end{array}\right\} \tag{2.3c}$$

$$\boldsymbol{D} = \left[\begin{array}{cc} E(y) & 0 \\ 0 & G(y) \end{array}\right] \tag{2.3d}$$

where:

$$\boldsymbol{E_1} = \boldsymbol{I} = \begin{bmatrix} 1 & 0 \\ 0 & 1 \end{bmatrix} \tag{2.4a}$$

$$\boldsymbol{E_2} = \begin{bmatrix} 0 & 1 \\ 0 & 0 \end{bmatrix} \tag{2.4b}$$

2.2 Derivation of beam governing equations

2.2.1 VWP based equations I

We try to develop beam governing equation starting from equation (1.10) that adopting the notation just introduced becomes:

$$-\int_{\Omega} \delta \boldsymbol{s}^T \left(\boldsymbol{L}\boldsymbol{D}\boldsymbol{L}^T \boldsymbol{s} + \boldsymbol{f} \right) d\Omega + \tag{2.5a}$$

$$\int_{\partial\Omega_t} \delta \boldsymbol{s}^T \left(\boldsymbol{N} \left(\boldsymbol{D}\boldsymbol{L}^T \boldsymbol{s} \right) - \boldsymbol{t} \right) dS = 0 \tag{2.5b}$$

Term (2.5a) is defined in the body while term (2.5b) is defined on the force boundary. Obviously to satisfy the stationarity condition both of them must be null.
In the following subsections we develop them individually.

Body equations

We re-write the body defined integral (2.5a) splitting vectors and matrix components:

$$\begin{gathered} -\int_{\Omega} \left[\delta \boldsymbol{u}^T \boldsymbol{p_u}, \delta \boldsymbol{v}^T \boldsymbol{p_v} \right] \left(\left[\frac{\partial}{\partial x} \boldsymbol{E_1} + \frac{\partial}{\partial y} \boldsymbol{E_2} \right] \begin{bmatrix} E & 0 \\ 0 & G \end{bmatrix} \right. \\ \left. \left[\frac{\partial}{\partial x} \boldsymbol{E_1} + \frac{\partial}{\partial y} \boldsymbol{E_2}^T \right] \left\{ \begin{array}{c} \boldsymbol{p_u}^T \boldsymbol{u} \\ \boldsymbol{p_v}^T \boldsymbol{v} \end{array} \right\} + \left\{ \begin{array}{c} f_x \\ f_y \end{array} \right\} \right) d\Omega = 0 \end{gathered} \tag{2.6}$$

If we develop the matrix products, the derivatives and collect all the basis terms in the resultant matrices we obtain:

$$\begin{gathered} -\int_{\Omega} \left[\delta \boldsymbol{u}^T, \delta \boldsymbol{v}^T \right] \left(\begin{bmatrix} \boldsymbol{p_u} E \boldsymbol{p_u}^T & 0 \\ 0 & \boldsymbol{p_v} G \boldsymbol{p_v}^T \end{bmatrix} \left\{ \begin{array}{c} \boldsymbol{u}'' \\ \boldsymbol{v}'' \end{array} \right\} + \right. \\ \begin{bmatrix} 0 & \boldsymbol{p_u} G \boldsymbol{p_v}'^T \\ \boldsymbol{p_v} G \boldsymbol{p_u}'^T & 0 \end{bmatrix} \left\{ \begin{array}{c} \boldsymbol{u}' \\ \boldsymbol{v}' \end{array} \right\} + \\ \left. \begin{bmatrix} \boldsymbol{p_u} G \boldsymbol{p_u}''^T & 0 \\ 0 & 0 \end{bmatrix} \left\{ \begin{array}{c} \boldsymbol{u} \\ \boldsymbol{v} \end{array} \right\} + \left\{ \begin{array}{c} \boldsymbol{p_u} f_x \\ \boldsymbol{p_v} f_y \end{array} \right\} \right) d\Omega = 0 \end{gathered} \tag{2.7}$$

Terms inside matrices depend only on y, on the opposite terms over the matrices depend only on the axial variable, so we can write the volume integral as the double integral on the two sub-spaces constituting it: the section integral and in the axial integral. By the variable separation we obtain:

$$
\begin{gathered}
-\int_l [\delta \boldsymbol{u}^T, \delta \boldsymbol{v}^T] \left(\begin{bmatrix} \boldsymbol{P_{uu}} & \boldsymbol{0} \\ \boldsymbol{0} & \boldsymbol{P_{vv}} \end{bmatrix} \begin{Bmatrix} \boldsymbol{u}'' \\ \boldsymbol{v}'' \end{Bmatrix} + \right. \\
\left. \begin{bmatrix} \boldsymbol{0} & \boldsymbol{P_{uv'}} \\ \boldsymbol{P_{vu'}} & \boldsymbol{0} \end{bmatrix} \begin{Bmatrix} \boldsymbol{u}' \\ \boldsymbol{v}' \end{Bmatrix} + \begin{bmatrix} \boldsymbol{P_{uu''}} & \boldsymbol{0} \\ \boldsymbol{0} & \boldsymbol{0} \end{bmatrix} \begin{Bmatrix} \boldsymbol{u} \\ \boldsymbol{v} \end{Bmatrix} + \begin{Bmatrix} \boldsymbol{F_x} \\ \boldsymbol{F_y} \end{Bmatrix} \right) dx = 0
\end{gathered}
\tag{2.8}
$$

in which:

$$
\begin{aligned}
\boldsymbol{P_{uu}} &= \int_A \boldsymbol{p_u} E \boldsymbol{p_u}^T dA & \boldsymbol{P_{vv}} &= \int_A \boldsymbol{p_v} G \boldsymbol{p_v}^T dA \\
\boldsymbol{P_{uv'}} &= \int_A \boldsymbol{p_u} G \boldsymbol{p_v}'^T dA & \boldsymbol{P_{vu'}} &= \int_A \boldsymbol{p_v} G \boldsymbol{p_u}'^T dA \\
\boldsymbol{P_{uu''}} &= \int_A \boldsymbol{p_u} G \boldsymbol{p_u}''^T dA & & \\
\boldsymbol{F_x} &= \int_A \boldsymbol{p_u} f_x dA & \boldsymbol{F_y} &= \int_A \boldsymbol{p_v} f_y dA
\end{aligned}
\tag{2.9}
$$

The equivalent strong formulation of the problem can be expressed as follows:

$$
\boldsymbol{P_{uu}} \boldsymbol{u}'' + \boldsymbol{P_{uv'}} \boldsymbol{v}' + \boldsymbol{P_{uu''}} \boldsymbol{u} + \boldsymbol{F_x} = 0 \tag{2.10a}
$$

$$
\boldsymbol{P_{vv}} \boldsymbol{v}'' + \boldsymbol{P_{vu'}} \boldsymbol{u}' + \boldsymbol{F_y} = 0 \tag{2.10b}
$$

Using a more compact notation we can write:

$$
\boldsymbol{P} \hat{\boldsymbol{s}}'' + \boldsymbol{Q} \hat{\boldsymbol{s}}' + \boldsymbol{R} \hat{\boldsymbol{s}} + \boldsymbol{F} = 0 \tag{2.11}
$$

in which

$$
\begin{aligned}
\boldsymbol{P} &= \begin{bmatrix} \boldsymbol{P_{uu}} & \boldsymbol{0} \\ \boldsymbol{0} & \boldsymbol{P_{vv}} \end{bmatrix} & \boldsymbol{Q} &= \begin{bmatrix} \boldsymbol{0} & \boldsymbol{P_{uv'}} \\ \boldsymbol{P_{vu'}} & \boldsymbol{0} \end{bmatrix} \\
\boldsymbol{R} &= \begin{bmatrix} \boldsymbol{P_{uu''}} & \boldsymbol{0} \\ \boldsymbol{0} & \boldsymbol{0} \end{bmatrix} & \boldsymbol{F} &= \begin{Bmatrix} \boldsymbol{F_x} \\ \boldsymbol{F_y} \end{Bmatrix}
\end{aligned}
\tag{2.12}
$$

Force boundary equations

To facilitate the development of the force boundary term we make some hypotheses, in particular we suppose that we are working on a cantilever, clamped at the origin of the axis and loaded at the opposite section. We suppose also that on the lateral surface of the beam no load is applied:

$$
\partial \Omega_t \equiv A_l \cup S_{\pm \frac{h}{2}} \tag{2.13a}
$$

$$
\boldsymbol{t}(A_l) = \begin{Bmatrix} 0 \\ t_y \end{Bmatrix} \qquad \boldsymbol{t}(S_{\pm \frac{h}{2}}) = \begin{Bmatrix} 0 \\ 0 \end{Bmatrix} \tag{2.13b}
$$

Obviously these choices are conventional, in every moment we can change them and develop other kinds of constraint even if the development is always the same.

Splitting components in term (2.5b) we can write:

$$\int_{\partial\Omega_t} [\delta\boldsymbol{u}^T, \delta\boldsymbol{v}^T] \left(\begin{bmatrix} n_x & n_y \\ 0 & n_x \end{bmatrix} \begin{bmatrix} E & 0 \\ 0 & G \end{bmatrix} \left[\frac{\partial}{\partial x}\boldsymbol{E_1} + \frac{\partial}{\partial y}\boldsymbol{E_2}^T \right] \left\{ \begin{array}{c} \boldsymbol{p_u}^T \boldsymbol{u} \\ \boldsymbol{p_v}^T \boldsymbol{v} \end{array} \right\} - \left\{ \begin{array}{c} t_x \\ t_y \end{array} \right\} \right) dS = 0 \tag{2.14}$$

Developing the products and collecting the base functions in the resultant matrices we obtain:

$$\begin{aligned} &\int_{\partial\Omega_t} [\delta\boldsymbol{u}^T, \delta\boldsymbol{v}^T] \left(\begin{bmatrix} \boldsymbol{p_u} E n_x \boldsymbol{p_u}^T & \boldsymbol{p_u} G n_y \boldsymbol{p_v}^T \\ 0 & \boldsymbol{p_v} G n_x \boldsymbol{p_v}^T \end{bmatrix} \left\{ \begin{array}{c} \boldsymbol{u}' \\ \boldsymbol{v}' \end{array} \right\} + \right. \\ &\left. \begin{bmatrix} \boldsymbol{p_u} G n_y \boldsymbol{p_u}'^T & 0 \\ \boldsymbol{p_v} G n_x \boldsymbol{p_u}'^T & 0 \end{bmatrix} \left\{ \begin{array}{c} \boldsymbol{u} \\ \boldsymbol{v} \end{array} \right\} - \left\{ \begin{array}{c} t_x \\ t_y \end{array} \right\} \right) dA = 0 \end{aligned} \tag{2.15}$$

Now we decompose the integral domain in the sub - regions constituting the force boundary.

$$\begin{aligned} &\int_A [\delta\boldsymbol{u}(l)^T, \delta\boldsymbol{v}(l)^T] \left(\begin{bmatrix} \boldsymbol{p_u} E \boldsymbol{p_u}^T & 0 \\ 0 & \boldsymbol{p_v} G \boldsymbol{p_v}^T \end{bmatrix} \left\{ \begin{array}{c} \boldsymbol{u}'(l) \\ \boldsymbol{v}'(l) \end{array} \right\} + \right. \\ &\qquad \left. \begin{bmatrix} 0 & 0 \\ \boldsymbol{p_v} G \boldsymbol{p_u}'^T & 0 \end{bmatrix} \left\{ \begin{array}{c} \boldsymbol{u}(l) \\ \boldsymbol{v}(l) \end{array} \right\} - \left\{ \begin{array}{c} \boldsymbol{p_u} t_x \\ \boldsymbol{p_v} t_y \end{array} \right\} \right) dA + \\ &\int_l [\delta\boldsymbol{u}^T, \delta\boldsymbol{v}^T] \left(\begin{bmatrix} 0 & \boldsymbol{p_u}\left(\frac{h}{2}\right) G \boldsymbol{p_v}\left(\frac{h}{2}\right)^T \\ 0 & 0 \end{bmatrix} \left\{ \begin{array}{c} \boldsymbol{u}' \\ \boldsymbol{v}' \end{array} \right\} + \right. \\ &\qquad \left. \begin{bmatrix} \boldsymbol{p_u}\left(\frac{h}{2}\right) G \boldsymbol{p_u}'\left(\frac{h}{2}\right)^T & 0 \\ 0 & 0 \end{bmatrix} \left\{ \begin{array}{c} \boldsymbol{u} \\ \boldsymbol{v} \end{array} \right\} \right) dx - \\ &\int_l [\delta\boldsymbol{u}^T, \delta\boldsymbol{v}^T] \left(\begin{bmatrix} 0 & \boldsymbol{p_u}\left(-\frac{h}{2}\right) G \boldsymbol{p_v}\left(-\frac{h}{2}\right)^T \\ 0 & 0 \end{bmatrix} \left\{ \begin{array}{c} \boldsymbol{u}' \\ \boldsymbol{v}' \end{array} \right\} + \right. \\ &\qquad \left. \begin{bmatrix} \boldsymbol{p_u}\left(-\frac{h}{2}\right) G \boldsymbol{p_u}'\left(-\frac{h}{2}\right)^T & 0 \\ 0 & 0 \end{bmatrix} \left\{ \begin{array}{c} \boldsymbol{u} \\ \boldsymbol{v} \end{array} \right\} \right) dx = 0 \end{aligned} \tag{2.16}$$

Using a more compact notation we obtain:

$$\begin{aligned}&\Bigg([\delta\boldsymbol{u}^T,\delta\boldsymbol{v}^T]\Bigg(\begin{bmatrix}\boldsymbol{P_{uu}} & \boldsymbol{0}\\ \boldsymbol{0} & \boldsymbol{P_{vv}}\end{bmatrix}\begin{Bmatrix}\boldsymbol{u}'\\ \boldsymbol{v}'\end{Bmatrix}+\\&\begin{bmatrix}\boldsymbol{0} & \boldsymbol{0}\\ \boldsymbol{P_{vu'}} & \boldsymbol{0}\end{bmatrix}\begin{Bmatrix}\boldsymbol{u}\\ \boldsymbol{v}\end{Bmatrix}-\begin{Bmatrix}\boldsymbol{T_x}\\ \boldsymbol{T_y}\end{Bmatrix}\Bigg)\Bigg)\Bigg|_l+\\&\int_l \delta\boldsymbol{u}^T\left(\boldsymbol{p_u}G\boldsymbol{p_v}^T\boldsymbol{v}'+\boldsymbol{p_u}G\boldsymbol{p_u}'^T\boldsymbol{u}\right)dx\Bigg|_{\frac{h}{2}}-\\&\int_l \delta\boldsymbol{u}^T\left(\boldsymbol{p_u}G\boldsymbol{p_v}^T\boldsymbol{v}'+\boldsymbol{p_u}G\boldsymbol{p_u}'^T\boldsymbol{u}\right)dx\Bigg|_{-\frac{h}{2}}=0\end{aligned}\tag{2.17}$$

in which:

$$\boldsymbol{T_x}=\int_A \boldsymbol{p_u}t_x dA \qquad \boldsymbol{T_y}=\int_A \boldsymbol{p_v}t_y dA \tag{2.18}$$

The boundary conditions we obtain could be written in the following equivalent strong formulation:

$$\left(\begin{bmatrix}\boldsymbol{P_{uu}} & \boldsymbol{0}\\ \boldsymbol{0} & \boldsymbol{P_{vv}}\end{bmatrix}\begin{Bmatrix}\boldsymbol{u}'\\ \boldsymbol{v}'\end{Bmatrix}+\begin{bmatrix}\boldsymbol{0} & \boldsymbol{0}\\ \boldsymbol{P_{vu'}} & \boldsymbol{0}\end{bmatrix}\begin{Bmatrix}\boldsymbol{u}\\ \boldsymbol{v}\end{Bmatrix}-\begin{Bmatrix}\boldsymbol{T_x}\\ \boldsymbol{T_y}\end{Bmatrix}\right)\Bigg|_l=0 \tag{2.19a}$$

$$\left(\boldsymbol{p_u}G\boldsymbol{p_v}^T\boldsymbol{v}'+\boldsymbol{p_u}G\boldsymbol{p_u}'^T\boldsymbol{u}\right)\big|_{\frac{h}{2}}=0 \tag{2.19b}$$

$$\left(\boldsymbol{p_u}G\boldsymbol{p_v}^T\boldsymbol{v}'+\boldsymbol{p_u}G\boldsymbol{p_u}'^T\boldsymbol{u}\right)\big|_{-\frac{h}{2}}=0 \tag{2.19c}$$

Equations (2.19b) and (2.19c) can be re-write more clearly as follow:

$$\left(\boldsymbol{p_v}\boldsymbol{v'}+\boldsymbol{p_u}'\boldsymbol{u}\right)\big|_{\pm\frac{h}{2}}=0 \tag{2.20}$$

Displacement boundary equations

We must impose the compatibility condition on $\partial\Omega_s$, this last condition must be imposed in strong way, in other words, in the specific case we are considering, we must require that:

$$\begin{Bmatrix}\boldsymbol{u}\\ \boldsymbol{v}\end{Bmatrix}\Bigg|_0=\begin{Bmatrix}\boldsymbol{0}\\ \boldsymbol{0}\end{Bmatrix} \tag{2.21}$$

2.2.2 VWP based equations II

Adopting the notation introduced in 2.1 and adopting the same boundary conditions used in the previous section, WVP as expressed in (1.7) becomes:

$$\int_\Omega \left(\boldsymbol{L}^T\delta\boldsymbol{s}\right)^T\boldsymbol{D}\boldsymbol{L}^T\boldsymbol{s}d\Omega+\int_\Omega \delta\boldsymbol{s}^T\boldsymbol{f}d\Omega-\int_{\partial\Omega_t}\delta\boldsymbol{s}^T\boldsymbol{t}\,dS=0 \tag{2.22}$$

We re-write equation splitting vectors and matrix components:

$$\int_\Omega \left(\left[\frac{\partial}{\partial x}\boldsymbol{E_1} + \frac{\partial}{\partial y}\boldsymbol{E_2}^T \right] \left\{ \begin{array}{c} \boldsymbol{p_u}^T \delta\boldsymbol{u} \\ \boldsymbol{p_v}^T \delta\boldsymbol{v} \end{array} \right\} \right)^T \left[\begin{array}{cc} E & 0 \\ 0 & G \end{array} \right]$$
$$\left(\left[\frac{\partial}{\partial x}\boldsymbol{E_1} + \frac{\partial}{\partial y}\boldsymbol{E_2}^T \right] \left\{ \begin{array}{c} \boldsymbol{p_u}^T \boldsymbol{u} \\ \boldsymbol{p_v}^T \boldsymbol{v} \end{array} \right\} \right) d\Omega -$$
$$\int_\Omega [\delta\boldsymbol{u}^T\boldsymbol{p_u}, \delta\boldsymbol{v}^T\boldsymbol{p_v}] \left\{ \begin{array}{c} f_x \\ f_y \end{array} \right\} d\Omega - \int_{\partial\Omega_t} [\delta\boldsymbol{u}^T\boldsymbol{p_u}, \delta\boldsymbol{v}^T\boldsymbol{p_v}] \left\{ \begin{array}{c} t_x \\ t_y \end{array} \right\} dS = 0 \tag{2.23}$$

If we develop the matrix products and the derivatives, then we collect all the basis terms in resultant matrices we obtain:

$$\begin{aligned}
&\int_\Omega \Bigg(\left[\delta\boldsymbol{u}'^T, \delta\boldsymbol{v}'^T\right] \left[\begin{array}{cc} \boldsymbol{p_u} E \boldsymbol{p_u}^T & \boldsymbol{0} \\ \boldsymbol{0} & \boldsymbol{p_v} G \boldsymbol{p_v}^T \end{array} \right] \left\{ \begin{array}{c} \boldsymbol{u}' \\ \boldsymbol{v}' \end{array} \right\} + \\
&\left[\delta\boldsymbol{u}^T, \delta\boldsymbol{v}^T\right] \left[\begin{array}{cc} \boldsymbol{0} & \boldsymbol{p'_u} E \boldsymbol{p_v}^T \\ \boldsymbol{p_v} G \boldsymbol{p'_u}^T & \boldsymbol{0} \end{array} \right] \left\{ \begin{array}{c} \boldsymbol{u}' \\ \boldsymbol{v}' \end{array} \right\} + \\
&\left[\delta\boldsymbol{u}^T, \delta\boldsymbol{v}^T\right] \left[\begin{array}{cc} \boldsymbol{p'_u} E \boldsymbol{p'_u}^T & \boldsymbol{0} \\ \boldsymbol{0} & \boldsymbol{0} \end{array} \right] \left\{ \begin{array}{c} \boldsymbol{u} \\ \boldsymbol{v} \end{array} \right\} - \\
&\left[\delta\boldsymbol{u}^T, \delta\boldsymbol{v}^T\right] \left\{ \begin{array}{c} \boldsymbol{p_u} f_x \\ \boldsymbol{p_v} f_y \end{array} \right\} \Bigg) d\Omega - \\
&\int_{\partial\Omega_t} \left[\delta\boldsymbol{u}^T, \delta\boldsymbol{v}^T\right] \left\{ \begin{array}{c} \boldsymbol{p_u} t_x \\ \boldsymbol{p_v} t_y \end{array} \right\} dS = 0
\end{aligned} \tag{2.24}$$

Terms inside matrices depend only on the section variables, on the opposite terms over the matrices depend only on the axial variable, hence, as we previously do we can subdivide the integral domine in the sub-domines section and axis obtaining:

$$\int_l \Bigg(\left[\delta\boldsymbol{u}'^T, \delta\boldsymbol{v}'^T\right] \left[\begin{array}{cc} \boldsymbol{P_{uu}} & \boldsymbol{0} \\ \boldsymbol{0} & \boldsymbol{P_{vv}} \end{array} \right] \left\{ \begin{array}{c} \boldsymbol{u}' \\ \boldsymbol{v}' \end{array} \right\} + \tag{2.25a}$$
$$\left[\delta\boldsymbol{u}^T, \delta\boldsymbol{v}^T\right] \left[\begin{array}{cc} \boldsymbol{0} & \boldsymbol{P_{u'v}} \\ \boldsymbol{P_{vu'}} & \boldsymbol{0} \end{array} \right] \left\{ \begin{array}{c} \boldsymbol{u}' \\ \boldsymbol{v}' \end{array} \right\} + \tag{2.25b}$$
$$\left[\delta\boldsymbol{u}^T, \delta\boldsymbol{v}^T\right] \left[\begin{array}{cc} \boldsymbol{P_{u'u'}} & \boldsymbol{0} \\ \boldsymbol{0} & \boldsymbol{0} \end{array} \right] \left\{ \begin{array}{c} \boldsymbol{u} \\ \boldsymbol{v} \end{array} \right\} - \tag{2.25c}$$
$$\left[\delta\boldsymbol{u}^T, \delta\boldsymbol{v}^T\right] \left\{ \begin{array}{c} \boldsymbol{F_x} \\ \boldsymbol{F_y} \end{array} \right\} \Bigg) dx - \tag{2.25d}$$
$$\int_{\partial\Omega_t} \left[\delta\boldsymbol{u}^T, \delta\boldsymbol{v}^T\right] \left\{ \begin{array}{c} \boldsymbol{T_x} \\ \boldsymbol{T_y} \end{array} \right\} dS = 0 \tag{2.25e}$$

in which additionally to what we have already defined in (2.9) and in (2.18) we must define:

$$\boldsymbol{P_{u'v}} = \int_A \boldsymbol{p_u}' G \boldsymbol{p_v}^T dA \qquad \boldsymbol{P_{u'u'}} = \int_A \boldsymbol{p_u}' G \boldsymbol{p_u}'^T dA \tag{2.26a}$$

At this point we integrate by parts term (2.25a), supposing to working on the cantilever we obtain the final formulation of the problem:

$$\int_l \Bigg(-\left[\delta\boldsymbol{u}^T, \delta\boldsymbol{v}^T\right] \begin{bmatrix} \boldsymbol{P_{uu}} & \boldsymbol{0} \\ \boldsymbol{0} & \boldsymbol{P_{vv}} \end{bmatrix} \begin{Bmatrix} \boldsymbol{u}'' \\ \boldsymbol{v}'' \end{Bmatrix} + \tag{2.27a}$$

$$\left[\delta\boldsymbol{u}^T, \delta\boldsymbol{v}^T\right] \begin{bmatrix} \boldsymbol{0} & \boldsymbol{P_{u'v}} \\ \boldsymbol{P_{vu'}} & \boldsymbol{0} \end{bmatrix} \begin{Bmatrix} \boldsymbol{u}' \\ \boldsymbol{v}' \end{Bmatrix} + \tag{2.27b}$$

$$\left[\delta\boldsymbol{u}^T, \delta\boldsymbol{v}^T\right] \begin{bmatrix} \boldsymbol{P_{u'u'}} & \boldsymbol{0} \\ \boldsymbol{0} & \boldsymbol{0} \end{bmatrix} \begin{Bmatrix} \boldsymbol{u} \\ \boldsymbol{v} \end{Bmatrix} - \tag{2.27c}$$

$$\left[\delta\boldsymbol{u}^T, \delta\boldsymbol{v}^T\right] \begin{Bmatrix} \boldsymbol{F_x} \\ \boldsymbol{F_y} \end{Bmatrix} \Bigg) dx + \tag{2.27d}$$

$$\left(\left[\delta\boldsymbol{u}^T, \delta\boldsymbol{v}^T\right] \begin{bmatrix} \boldsymbol{P_{uu}} & \boldsymbol{0} \\ \boldsymbol{0} & \boldsymbol{P_{vv}} \end{bmatrix} \begin{Bmatrix} \boldsymbol{u}' \\ \boldsymbol{v}' \end{Bmatrix} - \begin{Bmatrix} \boldsymbol{T_x} \\ \boldsymbol{T_y} \end{Bmatrix} \right) \Bigg|_l = 0 \tag{2.27e}$$

The equivalent formulation of the problem is:

$$-\boldsymbol{P_{uu}}\boldsymbol{u}'' + \boldsymbol{Q_{u'v}}\boldsymbol{v}' + \boldsymbol{R_{u'u'}}\boldsymbol{u} - \boldsymbol{F_x} = \boldsymbol{0} \tag{2.28a}$$

$$-\boldsymbol{P_{vv}}\boldsymbol{v}'' + \boldsymbol{Q_{vu'}}\boldsymbol{u}' - \boldsymbol{F_y} = \boldsymbol{0} \quad \text{in}\Omega \tag{2.28b}$$

$$\boldsymbol{P_{uu}}\boldsymbol{u}' - \boldsymbol{T_x} = \boldsymbol{0} \tag{2.28c}$$

$$\boldsymbol{P_{vv}}\boldsymbol{v}' - \boldsymbol{T_y} = \boldsymbol{0} \quad \text{in}A \tag{2.28d}$$

That using a less compact notation we can write as:

$$\begin{aligned} -\boldsymbol{P}\hat{\boldsymbol{s}}'' + \boldsymbol{Q}\hat{\boldsymbol{s}}' + \boldsymbol{R}\hat{\boldsymbol{s}} - \boldsymbol{F} &= 0 \quad \text{in}\Omega \\ \boldsymbol{P}\hat{\boldsymbol{s}}' - \boldsymbol{T} &= 0 \quad \text{in}A_l \end{aligned} \tag{2.29}$$

in which

$$\boldsymbol{P} = \begin{bmatrix} \boldsymbol{P_{uu}} & \boldsymbol{0} \\ \boldsymbol{0} & \boldsymbol{P_{vv}} \end{bmatrix} \qquad \boldsymbol{Q} = \begin{bmatrix} \boldsymbol{0} & \boldsymbol{P_{u'v}} \\ \boldsymbol{P_{vu'}} & \boldsymbol{0} \end{bmatrix}$$

$$\boldsymbol{R} = \begin{bmatrix} \boldsymbol{P_{u'u'}} & \boldsymbol{0} \\ \boldsymbol{0} & \boldsymbol{0} \end{bmatrix} \qquad \boldsymbol{F} = \begin{Bmatrix} \boldsymbol{F_x} \\ \boldsymbol{F_y} \end{Bmatrix} \tag{2.30}$$

$$\boldsymbol{T} = \begin{Bmatrix} \boldsymbol{T_x} \\ \boldsymbol{T_y} \end{Bmatrix}$$

2.2.3 HR based equations

Adopting the notation defined in section 2.1 the HR stationarity condition (1.14) becomes:

$$\int_\Omega \delta\boldsymbol{\sigma}^T \left(\boldsymbol{L}^T\boldsymbol{s} - \boldsymbol{D}^{-1}\boldsymbol{\sigma}\right) d\Omega - \int_\Omega \delta\boldsymbol{s}^T \left(\boldsymbol{L}\boldsymbol{\sigma} + \boldsymbol{f}\right) d\Omega + \tag{2.31a}$$

$$\int_{\partial\Omega_t} \delta\boldsymbol{s}^T \left(\boldsymbol{N}\boldsymbol{\sigma} - \boldsymbol{t}\right) dS - \tag{2.31b}$$

$$\int_{\partial\Omega_s} \delta\boldsymbol{\sigma}^T \boldsymbol{N}^T \left(\boldsymbol{s} - \bar{\boldsymbol{s}}\right) dS = 0 \tag{2.31c}$$

In which we split the terms of the equation considering the integration domain. Integral terms (2.31a) are defined on the body, (2.31b) is defined on the force boundary and (2.31c) is defined on the displacements constrained surface. Obviously to satisfy the stationarity condition every term of (2.31) must be null. In the following we develop them separately.

Body equations

We rewrite the body terms (2.31a) splitting vector and matrix components.

$$\int_\Omega [\delta\boldsymbol{\sigma_x}^T\boldsymbol{p_\sigma}, \delta\boldsymbol{\tau}^T\boldsymbol{p_\tau}]\left(\left(\frac{\partial}{\partial x}\boldsymbol{E_1} + \frac{\partial}{\partial y}\boldsymbol{E_2}^T\right)\left\{\begin{array}{c}\boldsymbol{p_u}^T\boldsymbol{u}\\ \boldsymbol{p_v}^T\boldsymbol{v}\end{array}\right\} - \boldsymbol{D}^{-1}\left\{\begin{array}{c}\boldsymbol{p_\sigma}^T\boldsymbol{\sigma_x}\\ \boldsymbol{p_\tau}^T\boldsymbol{\tau}\end{array}\right\}\right)d\Omega -$$
$$\int_\Omega [\delta\boldsymbol{u}^T\boldsymbol{p_u}, \delta\boldsymbol{v}^T\boldsymbol{p_v}]\left(\left(\frac{\partial}{\partial x}\boldsymbol{E_1} + \frac{\partial}{\partial y}\boldsymbol{E_2}\right)\left\{\begin{array}{c}\boldsymbol{p_\sigma}^T\boldsymbol{\sigma_x}\\ \boldsymbol{p_\tau}^T\boldsymbol{\tau}\end{array}\right\} + \left\{\begin{array}{c}f_x\\ f_y\end{array}\right\}\right)d\Omega = 0 \tag{2.32}$$

Applying differential operators to the vectors, splitting unknow vectors and moving the base vectors inside the matrices, we obtain:

$$\begin{aligned}
&\int_\Omega [\delta\boldsymbol{\sigma_x}^T, \delta\boldsymbol{\tau}^T]\left(\begin{bmatrix}\boldsymbol{p_\sigma}\boldsymbol{p_u}^T & \mathbf{0}\\ \mathbf{0} & \boldsymbol{p_\tau}\boldsymbol{p_v^T}\end{bmatrix}\left\{\begin{array}{c}\boldsymbol{u}'\\ \boldsymbol{v}'\end{array}\right\} + \right.\\
&\left.\begin{bmatrix}\mathbf{0} & \mathbf{0}\\ \boldsymbol{p_\tau}\boldsymbol{p_u'}^T & \mathbf{0}\end{bmatrix}\left\{\begin{array}{c}\boldsymbol{u}\\ \boldsymbol{v}\end{array}\right\} - \begin{bmatrix}\dfrac{\boldsymbol{p_\sigma}\boldsymbol{p_\sigma}^T}{E} & \mathbf{0}\\ \mathbf{0} & \dfrac{\boldsymbol{p_\tau}\boldsymbol{p_\tau}}{G}\end{bmatrix}\left\{\begin{array}{c}\boldsymbol{\sigma_x}\\ \boldsymbol{\tau}\end{array}\right\}\right)d\Omega -\\
&\int_\Omega [\delta\boldsymbol{u}^T, \delta\boldsymbol{v}^T]\left(\begin{bmatrix}\boldsymbol{p_u}\boldsymbol{p_\sigma}^T & \mathbf{0}\\ \mathbf{0} & \boldsymbol{p_v}\boldsymbol{p_\tau}^T\end{bmatrix}\left\{\begin{array}{c}\boldsymbol{\sigma_x}'\\ \boldsymbol{\tau}'\end{array}\right\} + \right.\\
&\left.\begin{bmatrix}\mathbf{0} & \boldsymbol{p_u}\boldsymbol{p_\tau'}^T\\ \mathbf{0} & \mathbf{0}\end{bmatrix}\left\{\begin{array}{c}\boldsymbol{\sigma_x}\\ \boldsymbol{\tau}\end{array}\right\} + \left\{\begin{array}{c}\boldsymbol{p_u}f_x\\ \boldsymbol{p_v}f_y\end{array}\right\}\right)d\Omega = 0
\end{aligned} \tag{2.33}$$

It is possible to decompose the integral domain in the 2 sub-spaces, in fact only terms in the matrices depend on section variables and vector terms depend only on axial variable, the weak governing equations we are developing becomes:

$$\begin{aligned}
&\int_l [\delta\boldsymbol{\sigma_x}^T, \delta\boldsymbol{\tau}^T]\left(\begin{bmatrix}\boldsymbol{P_{\sigma u}} & \mathbf{0}\\ \mathbf{0} & \boldsymbol{P_{\tau v}}\end{bmatrix}\left\{\begin{array}{c}\boldsymbol{u}'\\ \boldsymbol{v}'\end{array}\right\} + \right.\\
&\left.\begin{bmatrix}\mathbf{0} & \mathbf{0}\\ \boldsymbol{P_{\tau u'}} & \mathbf{0}\end{bmatrix}\left\{\begin{array}{c}\boldsymbol{u}\\ \boldsymbol{v}\end{array}\right\} - \begin{bmatrix}\boldsymbol{P_{\sigma\sigma}} & \mathbf{0}\\ \mathbf{0} & \boldsymbol{P_{\tau\tau}}\end{bmatrix}\left\{\begin{array}{c}\boldsymbol{\sigma_x}\\ \boldsymbol{\tau}\end{array}\right\}\right)dx -\\
&\int_l [\delta\boldsymbol{u}^T, \delta\boldsymbol{v}^T]\left(\begin{bmatrix}\boldsymbol{P_{u\sigma}} & \mathbf{0}\\ \mathbf{0} & \boldsymbol{P_{v\tau}}\end{bmatrix}\left\{\begin{array}{c}\boldsymbol{\sigma_x}'\\ \boldsymbol{\tau}'\end{array}\right\} + \right.\\
&\left.\begin{bmatrix}\mathbf{0} & \boldsymbol{P_{u\tau'}}^T\\ \mathbf{0} & \mathbf{0}\end{bmatrix}\left\{\begin{array}{c}\boldsymbol{\sigma_x}\\ \boldsymbol{\tau}\end{array}\right\} + \left\{\begin{array}{c}\boldsymbol{F_x}\\ \boldsymbol{F_y}\end{array}\right\}\right)dx = 0
\end{aligned} \tag{2.34}$$

in which we define the follow matrices:

$$
\begin{aligned}
\boldsymbol{P_{\sigma u}} &= \int_A \boldsymbol{p_\sigma} \boldsymbol{p_u}^T \, dA & \boldsymbol{P_{\tau v}} &= \int_A \boldsymbol{p_\tau} \boldsymbol{p_v}^T \, dA \\
\boldsymbol{P_{u\sigma}} &= \int_A \boldsymbol{p_u} \boldsymbol{p_\sigma}^T \, dA & \boldsymbol{P_{v\tau}} &= \int_A \boldsymbol{p_v} \boldsymbol{p_\tau}^T \, dA \\
\boldsymbol{P_{\sigma\sigma}} &= \int_A \frac{\boldsymbol{p_\sigma} \boldsymbol{p_\sigma}^T}{E} dA & \boldsymbol{P_{\tau\tau}} &= \int_A \frac{\boldsymbol{p_\tau} \boldsymbol{p_\tau}^T}{G} dA \\
\boldsymbol{P_{\tau u'}} &= \int_A \boldsymbol{p_\tau} \boldsymbol{p_u}'^T \, dA & \boldsymbol{P_{u\tau'}} &= \int_A \boldsymbol{p_u} \boldsymbol{p_\tau}'^T \, dA \\
\boldsymbol{F_x} &= \int_A \boldsymbol{p_u} f_x \, dA & \boldsymbol{F_y} &= \int_A \boldsymbol{p_v} f_y \, dA
\end{aligned}
\tag{2.35}
$$

The strong formulation of the problem could be express as:

$$\boldsymbol{P_{\sigma u}} \boldsymbol{u}' - \boldsymbol{P_{\sigma\sigma}} \boldsymbol{\sigma} = 0 \tag{2.36a}$$

$$\boldsymbol{P_{\tau v}} \boldsymbol{v}' + \boldsymbol{P_{\tau u'}} \boldsymbol{u} - \boldsymbol{P_{\tau\tau}} \boldsymbol{\tau} = 0 \tag{2.36b}$$

$$\boldsymbol{P_{u\sigma}} \boldsymbol{\sigma_x}' + \boldsymbol{P_{u\tau'}} \boldsymbol{\tau} + \boldsymbol{F_x} = 0 \tag{2.36c}$$

$$\boldsymbol{P_{v\tau}} \boldsymbol{\tau}' + \boldsymbol{F_y} = 0 \tag{2.36d}$$

Alternatively we can re-write the problem in a more compact notation. It results as follows:

$$\boldsymbol{A} \left\{ \begin{array}{c} \hat{\boldsymbol{\sigma}}' \\ \hat{\boldsymbol{s}}' \end{array} \right\} + \boldsymbol{G} \left\{ \begin{array}{c} \hat{\boldsymbol{\sigma}} \\ \hat{\boldsymbol{s}} \end{array} \right\} + \left\{ \begin{array}{c} \mathbf{0} \\ \boldsymbol{F} \end{array} \right\} = \mathbf{0} \tag{2.37}$$

in which

$$
\begin{aligned}
\hat{\boldsymbol{s}} &= \left\{ \begin{array}{c} \boldsymbol{u} \\ \boldsymbol{v} \end{array} \right\} & \hat{\boldsymbol{\sigma}} &= \left\{ \begin{array}{c} \boldsymbol{\sigma} \\ \boldsymbol{\tau} \end{array} \right\} \\
\boldsymbol{A} &= \left[\begin{array}{cccc} \mathbf{0} & \mathbf{0} & \boldsymbol{P_{\sigma u}} & \mathbf{0} \\ \mathbf{0} & \mathbf{0} & \mathbf{0} & \boldsymbol{P_{\tau v}} \\ \boldsymbol{P_{u\sigma}} & \mathbf{0} & \mathbf{0} & \mathbf{0} \\ \mathbf{0} & \boldsymbol{P_{v\tau}} & \mathbf{0} & \mathbf{0} \end{array} \right] & \boldsymbol{G} &= \left[\begin{array}{cccc} -\boldsymbol{P_{\sigma\sigma}} & \mathbf{0} & \mathbf{0} & \mathbf{0} \\ \mathbf{0} & -\boldsymbol{P_{\tau\tau}} & \boldsymbol{P_{\tau u'}} & \mathbf{0} \\ \mathbf{0} & \boldsymbol{P_{u\tau'}} & \mathbf{0} & \mathbf{0} \\ \mathbf{0} & \mathbf{0} & \mathbf{0} & \mathbf{0} \end{array} \right]
\end{aligned}
\tag{2.38}
$$

The problem, as we have just formulated it, can be reduced to an other, more simple formulation in which only displacements appear: this is possible noting that we can invert equations (2.36a) and (2.36b) and substitute the stress definition we obtain in equations (2.36c) and (2.36d). In other words:

$$\boldsymbol{\sigma} = \boldsymbol{P_{\sigma\sigma}}^{-1} \boldsymbol{P_{\sigma u}} \boldsymbol{u}' \tag{2.39a}$$

$$\boldsymbol{\tau} = \boldsymbol{P_{\tau\tau}}^{-1} \left(\boldsymbol{P_{\tau v}} \boldsymbol{v}' + \boldsymbol{P_{\tau u'}} \boldsymbol{u} \right) \tag{2.39b}$$

$$\boldsymbol{C_{uu}} \boldsymbol{u}'' + \boldsymbol{C_{uv}} \boldsymbol{v}' + \boldsymbol{C_{uu'}} \boldsymbol{u} + \boldsymbol{F_x} = 0 \tag{2.39c}$$

$$\boldsymbol{C_{vv}} \boldsymbol{v}'' + \boldsymbol{C_{vu}} \boldsymbol{u}' + \boldsymbol{F_y} = 0 \tag{2.39d}$$

in which:

$$\begin{aligned} &\boldsymbol{C_{uu}} = \boldsymbol{P_{u\sigma}}\boldsymbol{P_{\sigma\sigma}}^{-1}\boldsymbol{P_{\sigma u}} \quad && \boldsymbol{C_{uv}} = \boldsymbol{P_{u\tau'}}\boldsymbol{P_{\tau\tau}}^{-1}\boldsymbol{P_{\tau v}} \\ &\boldsymbol{C_{uu'}} = \boldsymbol{P_{u\tau'}}\boldsymbol{P_{\tau\tau}}^{-1}\boldsymbol{P_{\tau u'}} \quad && \boldsymbol{C_{vv}} = \boldsymbol{P_{v\tau}}\boldsymbol{P_{\tau\tau}}^{-1}\boldsymbol{P_{\tau v}} \\ &\boldsymbol{C_{vu}} = \boldsymbol{P_{v\tau}}\boldsymbol{P_{\tau\tau}}^{-1}\boldsymbol{P_{\tau u'}} \end{aligned} \tag{2.40}$$

Force boundary conditions

We suppose that the boundary conditions of the problem we are studying here are the same of 2.2.1.
Introducing the vectorial notation term (2.31b) became:

$$\begin{aligned} &\int_{\partial\Omega_t} \left[\delta\boldsymbol{u}^T\boldsymbol{p_u}, \delta\boldsymbol{v}^T\boldsymbol{p_v}\right] \left(\begin{bmatrix} n_x & n_y \\ 0 & n_x \end{bmatrix} \begin{Bmatrix} \boldsymbol{p_\sigma}^T\boldsymbol{\sigma_x} \\ \boldsymbol{p_\tau}^T\boldsymbol{\tau} \end{Bmatrix} - \begin{Bmatrix} t_x \\ t_y \end{Bmatrix} \right) dS = 0 \\ &\int_{\partial\Omega_t} \left[\delta\boldsymbol{u}^T, \delta\boldsymbol{v}^T\right] \left(\begin{bmatrix} n_x\boldsymbol{p_u}\boldsymbol{p_\sigma}^T & n_y\boldsymbol{p_u}\boldsymbol{p_\tau}^T \\ \boldsymbol{0} & n_x\boldsymbol{p_v}\boldsymbol{p_\tau}^T \end{bmatrix} \begin{Bmatrix} \boldsymbol{\sigma_x} \\ \boldsymbol{\tau} \end{Bmatrix} - \begin{Bmatrix} \boldsymbol{p_u}t_x \\ \boldsymbol{p_v}t_y \end{Bmatrix} \right) dS = 0 \end{aligned} \tag{2.41}$$

Considering now every beam surface we can split integrals and better define versors:

$$\begin{aligned} &\left(\left[\delta\boldsymbol{u}^T, \delta\boldsymbol{v}^T\right] \left(\begin{bmatrix} \boldsymbol{P_{u\sigma}}^T & \boldsymbol{0} \\ \boldsymbol{0} & \boldsymbol{P_{v\tau}}^T \end{bmatrix} \begin{Bmatrix} \boldsymbol{\sigma_x} \\ \boldsymbol{\tau} \end{Bmatrix} - \begin{Bmatrix} \boldsymbol{T_x} \\ \boldsymbol{T_y} \end{Bmatrix} \right) \right) \Bigg|_l + \\ &\int_l \left(\left[\delta\boldsymbol{u}^T, \delta\boldsymbol{v}^T\right] \begin{bmatrix} \boldsymbol{0} & -\boldsymbol{p_u}\boldsymbol{p_\tau}^T \\ \boldsymbol{0} & \boldsymbol{0} \end{bmatrix} \begin{Bmatrix} \boldsymbol{\sigma_x} \\ \boldsymbol{\tau} \end{Bmatrix} - \begin{Bmatrix} \boldsymbol{p_u}t_x \\ \boldsymbol{0} \end{Bmatrix} \right) dx \Bigg|_{-\frac{h}{2}} + \\ &\int_l \left(\left[\delta\boldsymbol{u}^T, \delta\boldsymbol{v}^T\right] \begin{bmatrix} \boldsymbol{0} & \boldsymbol{p_u}\boldsymbol{p_\tau}^T \\ \boldsymbol{0} & \boldsymbol{0} \end{bmatrix} \begin{Bmatrix} \boldsymbol{\sigma_x} \\ \boldsymbol{\tau} \end{Bmatrix} - \begin{Bmatrix} \boldsymbol{p_u}t_x \\ \boldsymbol{0} \end{Bmatrix} \right) dx \Bigg|_{\frac{h}{2}} \end{aligned} \tag{2.42}$$

in which we adopt the quantities previously defined (2.35) and (2.18). In strong way this means that:

$$\begin{bmatrix} \boldsymbol{P_{u\sigma}} & \boldsymbol{0} \\ \boldsymbol{0} & \boldsymbol{P_{v\tau}} \end{bmatrix} \begin{Bmatrix} \boldsymbol{\sigma_x} \\ \boldsymbol{\tau} \end{Bmatrix} \Bigg|_l - \begin{Bmatrix} \boldsymbol{T_x} \\ \boldsymbol{T_y} \end{Bmatrix} = \boldsymbol{0} \tag{2.43a}$$

$$\left(\boldsymbol{P}\boldsymbol{\tau} + \boldsymbol{p_u}t_x\right)\big|_{-\frac{h}{2}} \tag{2.43b}$$

$$\left(\boldsymbol{P}\boldsymbol{\tau} + \boldsymbol{p_u}t_x\right)\big|_{-\frac{h}{2}} \tag{2.43c}$$

in which:

$$\boldsymbol{P} = \boldsymbol{p_u}(\bar{y})\boldsymbol{p_\tau}(\bar{y})^T \tag{2.44}$$

Displacement bounded surface equations

Watching at hypotheses made in section 2.3 we have that:

$$\partial\Omega_s \equiv A_0 \tag{2.45a}$$

$$\bar{\boldsymbol{s}}(A_0) = \begin{Bmatrix} 0 \\ 0 \end{Bmatrix} \tag{2.45b}$$

To impose this condition in the model we must require that

$$
\begin{gathered}
\int_{\partial\Omega_s} \left[\delta\boldsymbol{\sigma_x}^T \boldsymbol{p_\sigma}, \delta\boldsymbol{\tau}^T \boldsymbol{p_\tau}\right] \left(\begin{bmatrix} n_x & 0 \\ n_y & n_x \end{bmatrix} \begin{Bmatrix} \boldsymbol{p_u}^T \boldsymbol{u} \\ \boldsymbol{p_v}^T \boldsymbol{v} \end{Bmatrix} + \begin{Bmatrix} \bar{u} \\ \bar{v} \end{Bmatrix} \right) dS = 0 \\
\int_{\partial\Omega_s} \left[\delta\boldsymbol{\sigma_x}^T, \delta\boldsymbol{\tau}^T\right] \left(\begin{bmatrix} n_x \boldsymbol{p_\sigma} \boldsymbol{p_u}^T & \boldsymbol{0} \\ n_y \boldsymbol{p_\tau} \boldsymbol{p_u}^T & n_x \boldsymbol{p_\tau} \boldsymbol{p_v}^T \end{bmatrix} \begin{Bmatrix} \boldsymbol{u} \\ \boldsymbol{v} \end{Bmatrix} + \begin{Bmatrix} \boldsymbol{p_\sigma} 0 \\ \boldsymbol{p_\tau} 0 \end{Bmatrix} \right) dS = 0 \\
\left(\left[\delta\boldsymbol{\sigma_x}^T, \delta\boldsymbol{\tau}^T\right] \left(\begin{bmatrix} -\boldsymbol{P_{\sigma u}} & \boldsymbol{0} \\ \boldsymbol{0} & -\boldsymbol{P_{\tau v}} \end{bmatrix} \begin{Bmatrix} \boldsymbol{u} \\ \boldsymbol{v} \end{Bmatrix} + \boldsymbol{0} \right) \right) \Bigg|_0 = 0
\end{gathered}
\tag{2.46}
$$

The equivalent strong formulation of this condition is:

$$
\begin{bmatrix} -\boldsymbol{P_{\sigma u}} & \boldsymbol{0} \\ \boldsymbol{0} & -\boldsymbol{P_{\tau v}} \end{bmatrix} \begin{Bmatrix} \boldsymbol{u} \\ \boldsymbol{v} \end{Bmatrix} \Bigg|_0 = \boldsymbol{0}
\tag{2.47}
$$

2.2.4 Conclusions on governing equations

The sets of governing equations we have just developed show many differences:

- In the first set of governing equations, since we apply the divergence theorem, it is possible to impose boundary equilibrium everywhere, also in the lateral surface.
- In the second set of equations, since we only integrate by parts in x direction, it is possible to impose boundary conditions only on surfaces with $n_x \neq 0$.
- Differently from the first set, the second shows a symmetric formulation.
- Even if the first formulation could appear better, trying to introduce the hypotheses of classical beams, it is not possible to obtain the correct equation, this happened using the second set.

2.3 Beam models

In this section we are going to develop some homogeneous beam models introducing field hypotheses in the governing equations we have derivated in section 2.2. In the following we illustrate the most common path used in literature (VWP) but also we try to obtain models using different one (HR). For every model we are going to develop we will make some numerical example to highlight differences between them.

Watching at the hypotheses we are using in this section we can consider E and G simply as scalar quantities

2.3.1 Timoshenko beam

Governing equation

To develop the Timoshenko beam we must introduce in the second set of equations (2.28) the follow hypotheses:

$$\boldsymbol{p_u} = \left\{ \begin{array}{c} 1 \\ y \end{array} \right\} \qquad \boldsymbol{p_v} = \{1\} \tag{2.48a}$$

$$\boldsymbol{u} = \left\{ \begin{array}{c} u_1 \\ u_2 \end{array} \right\} \qquad \boldsymbol{v} = \{v\} \tag{2.48b}$$

$$\boldsymbol{F} = \left\{ \begin{array}{c} F_{x1} \\ F_{x2} \\ F_y \end{array} \right\} \tag{2.48c}$$

As consequence the ODE system matrices can be evaluated, we report them in the follow:

$$\boldsymbol{P_{uu}} = \left[\begin{array}{cc} AE & 0 \\ 0 & IE \end{array} \right] \qquad \boldsymbol{P_{vv}} = [AG] \tag{2.49a}$$

$$\boldsymbol{Q_{vu'}} = \boldsymbol{Q_{u'v}}^T = \left[\begin{array}{cc} 0 & AG \end{array} \right] \qquad \boldsymbol{R_{u'u'}} = \left[\begin{array}{cc} 0 & 0 \\ 0 & AG \end{array} \right] \tag{2.49b}$$

So the beam governing equations became:

$$AEu_1'' = F_{x1} \tag{2.50a}$$

$$IEu_2'' + AG(v' + u_2) = F_{x2} \tag{2.50b}$$

$$AG(v'' + u_2') = F_y \tag{2.50c}$$

in which A and I are respectively the section area and second order static moment

$$A = bh \qquad I = \frac{bh^3}{12} \tag{2.51}$$

Shear factor

In the Timoshenko beam, to have a correct solution, we need to introduce in the constitutive relation some factors to equalize deformation works as obtained by the model and by the exact solution of the problem. In the Timoshenko beam the axial compression and the bending equations give a correct solution, so if we compare the exact deformation work and the deformation work obtained by the model, these are the same. About the shear, contrarily, we know that the model solution is approximated and it violates the boundary equilibrium, hence we aspect a factor unequal to 1, for this reason we must correct the τ constitutive relation as follows:

$$\tau = kG\gamma \tag{2.52}$$

Factor k can be estimated comparing the deformation works of Timoshenko and Jourawski beams.
The Jourawsky solution, where τ is parabolic, can be considered correct for a rectangular section so the exact work of shear deformation can be expressed as:

$$\mathcal{L}_J = b\int_{-h/2}^{h/2} \frac{\tau^2}{2G} dy = b\int_{-h/2}^{h/2} \frac{\left(\frac{6T(y^2-\frac{1}{4}h^2)}{bt^3}\right)^2}{2G} dy = \frac{3T^2}{5AG} \tag{2.53}$$

in which T is the resultant of shear stresses on the section.
In the Timoshenko model τ is constant on the section, so the work becomes:

$$\mathcal{L}_T = b\int_{-h/2}^{h/2} \frac{\tau^2}{2kG} dy = b\int_{-h/2}^{h/2} \frac{\left(\frac{T}{bh}\right)^2}{2kG} dy = \frac{T^2}{2AkG} \tag{2.54}$$

Equalizing these two works, we obtain, for the rectangular section, the following value of k:

$$\mathcal{L}_J = \mathcal{L}_T \quad \Longrightarrow \quad \frac{3T^2}{5AG} = \frac{T^2}{2AkG} \quad \Longrightarrow \quad k = \frac{5}{6} \tag{2.55}$$

We can observe that for the Timoshenko problem the shear factor depends only on section geometry and it's independent on the dimensions of the section and from the mechanical characteristics of the material. It's possible to demonstrate that the shear factor can not be higher than one ($k \leq 1$).

We can now rewrite the governing equations in the complete and correct way:

$$AEu_1'' = F_{x1} \tag{2.56a}$$

$$EIu_2'' + \frac{5}{6}AG(v' + u_2) = F_{x2} \tag{2.56b}$$

$$\frac{5}{6}AG(v'' + u_2') = F_y \tag{2.56c}$$

For the numerical example see section 2.3.3

2.3.2 Euler-Bernoulli beam

Governing equation

The fundamental hypothesis that permits to develop the Euler-Bernoulli beam is that shear deformation is negligible. This means that $\gamma = 0$ so, using the same notation we have already adopted previously $v' + u_2 = 0 so u_2 = v'$

substituting this hypothesis in equation (2.25) and using the matrices (2.49) we obtain:

$$\begin{aligned}
&\int_l -\left[\delta u_1, \delta v', \delta v\right] \left(\begin{bmatrix} AE & 0 & 0 \\ 0 & IE & 0 \\ 0 & 0 & AG \end{bmatrix} \begin{Bmatrix} u_1'' \\ v''' \\ v'' \end{Bmatrix} + \right.\\
&\begin{bmatrix} 0 & 0 & 0 \\ 0 & 0 & AG \\ 0 & AG & 0 \end{bmatrix} \begin{Bmatrix} u_1' \\ v'' \\ v' \end{Bmatrix} + \\
&\left. \begin{bmatrix} 0 & 0 & 0 \\ 0 & AG & 0 \\ 0 & 0 & 0 \end{bmatrix} \begin{Bmatrix} u_1' \\ v'' \\ v' \end{Bmatrix} - \begin{Bmatrix} F_{x1} \\ F_{x2} \\ F_y \end{Bmatrix} \right) dx + \\
&\left. \left(\left[\delta u_1, \delta v', \delta v\right] \begin{bmatrix} AE & 0 & 0 \\ 0 & IE & 0 \\ 0 & 0 & AG \end{bmatrix} \begin{Bmatrix} u_1' \\ v'' \\ v' \end{Bmatrix} - \begin{Bmatrix} T_{x1} \\ T_{x2} \\ T_y \end{Bmatrix} \right) \right|_l = 0
\end{aligned} \tag{2.57}$$

Developing the products in the body integrals we obtain:

$$\int_l -\delta u_1 \left(AE\, u_1'' - F_{x1}\right) dx + \tag{2.58a}$$

$$\int_l \delta v' \left(-IE\, v''' + AG\, v' - AG\, v'\right) dx + \tag{2.58b}$$

$$\int_l \delta v \left(+AG\, v'' - AG\, v'' - F_y\right) dx \tag{2.58c}$$

$$\tag{2.58d}$$

Integrating by parts term (2.58b) and summing to term (2.58c) we obtain:

$$-\,\delta v \left(-IE\, v'''\right) |_0^l + \tag{2.59a}$$

$$\int_\Omega \delta v \left(IE\, v^{IV} - F_y\right) d\Omega \tag{2.59b}$$

$$\tag{2.59c}$$

The governing equations are:

$$AEu_1'' = F_{x1} \tag{2.60a}$$

$$IE\, v^{IV} = F_y \tag{2.60b}$$

2.3.3 Timoshenko/Jourawsky beam

The first test we will make is to introduce y - linear horizontal displacements and axial stress, quadratic shear stress and constant transversal displacements in the previous differential equations and see if it's possible to obtain the shear-factor corrected Timoshenko beam.

The name we assign to this model (from now TJ) depends on the statement that displacements and axial stresses are the classical of Timoshenko beam, contrarily the parabolic shear distribution come from the Jourawski theory. If we do not obtain this result we can not hope that using more complex fields the model we develop give a improved solution respect to the classical models.

Hypotheses

Here we better specify the hypotheses we previously discuss and we introduce also numerical value for quantities we are using, this last to make numerical examples in the following.

We try to develop the model for a beam (length $l = 10$) made by homogeneous material ($E = 10^5, G = 4 \cdot 10^4$).We impose also that $h = 1$ and $b = 1$.
The field basis we choose are the following:

$$\boldsymbol{p_u} = \boldsymbol{p_\sigma} = \left\{ \begin{array}{c} 1 \\ y \end{array} \right\} \tag{2.61a}$$

$$\boldsymbol{p_v} = \{1\} \qquad\qquad \boldsymbol{p_\tau} = \left\{1 - 4y^2\right\} \tag{2.61b}$$

We could use a more general basis to describe the shear but, in every case, imposing equations (2.43b), (2.43c) we obtain newly the base we have already adopted, in other words, choosing shear base we are imposing in strong way lateral surface boundary conditions.
It could be interesting to note that, in the case we are considering, even if we have chosen a more complex shear field we do not increase the degree of freedom respect to the Timoshenko beam.

About constrains and loads we suppose that the section is clamped at the origin and in the opposite section there is a transversal load of magnitude 1. In other words the boundary condition of the problem are:

$$\boldsymbol{u}(0) = \boldsymbol{0}; \qquad v(0) = 0; \qquad \boldsymbol{\sigma_x}(10) = \boldsymbol{0}; \qquad t_y(10) = \left\{ \begin{array}{c} 0 \\ -1 \end{array} \right\} \tag{2.62}$$

Governing equation

We must re-write equations (2.36) evaluating matrix terms. Introducing field hypotheses and numeric values in their definition we obtain:

$$\boldsymbol{P_{u\sigma}} = \boldsymbol{P_{\sigma u}} = \begin{bmatrix} 1 & 0 \\ 0 & \dfrac{1}{12} \end{bmatrix} \qquad \boldsymbol{P_{v\tau}} = \boldsymbol{P_{\tau v}} = \frac{2}{3} \tag{2.63a}$$

$$\boldsymbol{P_{\sigma\sigma}} = \begin{bmatrix} \dfrac{1}{E} & 0 \\ 0 & \dfrac{1}{12E} \end{bmatrix} \qquad \boldsymbol{P_{\tau\tau}} = \frac{8}{15G} \tag{2.63b}$$

$$\boldsymbol{P_{\tau u'}} = \boldsymbol{P_{u\tau'}}^T = \begin{bmatrix} 0 & \dfrac{2}{3} \end{bmatrix} \qquad \boldsymbol{F_x} = \mathbf{0} \qquad F_y = 0 \tag{2.63c}$$

About the boundary conditions, equations (2.43b) and (2.43c) are already satisfied so we must impose condition (2.43a) that became simply:

$$\boldsymbol{\tau}(l) = -\frac{3}{2} \tag{2.64}$$

At this point, to simplify the ODE system we can explicit $\boldsymbol{\sigma_x}$ from equation (2.36a) and $\boldsymbol{\tau}$ from equation (2.36b) and substitute them in equations (2.36c) and(2.36d), in this way we reduce our problem to a displacement formulation. This new formulation can be expressed as follows:

$$\boldsymbol{C_{uu}}\boldsymbol{u}'' + \boldsymbol{C_{uv}}\boldsymbol{v}' + \boldsymbol{C_{uu}}\boldsymbol{u} = 0 \tag{2.65a}$$

$$\boldsymbol{C_{vv}}\boldsymbol{v}'' + \boldsymbol{C_{vu}}\boldsymbol{u}' = 0 \tag{2.65b}$$

In which

$$\boldsymbol{C_{uu}} = \boldsymbol{P_{u\sigma}}\boldsymbol{P_{\sigma\sigma}}^{-1}\boldsymbol{P_{\sigma u}} = \begin{bmatrix} E & 0 \\ 0 & \dfrac{1}{12}E \end{bmatrix} \tag{2.66a}$$

$$\boldsymbol{C_{vv}} = \boldsymbol{P_{v\tau}}\boldsymbol{P_{\tau\tau}}^{-1}\boldsymbol{P_{\tau v}} = \frac{5}{6}G \tag{2.66b}$$

$$\boldsymbol{C_{uv}} = \boldsymbol{P_{u\tau'}}\boldsymbol{P_{\tau\tau}}^{-1}\boldsymbol{P_{\tau v}} = \begin{bmatrix} 0 \\ -\dfrac{5}{6}G \end{bmatrix} \tag{2.66c}$$

$$\boldsymbol{C_{vu}} = \boldsymbol{P_{v\tau}}\boldsymbol{P_{\tau\tau}}^{-1}\boldsymbol{P_{\tau u'}} = \begin{bmatrix} 0 & \dfrac{5}{6}G \end{bmatrix} \tag{2.66d}$$

$$\boldsymbol{C_{uu}} = \boldsymbol{P_{u\tau'}}\boldsymbol{P_{\tau\tau}}^{-1}\boldsymbol{P_{\tau u'}} = \begin{bmatrix} 0 & 0 \\ 0 & -\dfrac{5}{6}G \end{bmatrix} \tag{2.66e}$$

Writing in extensive way the ODE system we obtain:

$$Eu_1'' = 0 \tag{2.67a}$$

$$\frac{1}{12}Eu_2'' - \frac{5}{6}G(v' + u_2) = 0 \tag{2.67b}$$

$$\frac{5}{6}G(v'' + u_2') = 0 \tag{2.67c}$$

It is immediate to see that what we have just written are the Timoshenko governing equations in which the shear factor appears without introducing it as correction.
Imposing the boundary condition and solving the ODE we obtain the following solution:

$$\boldsymbol{u} = \left\{ \begin{array}{c} 0 \\ -6,00 \times 10^{-5}\, x^2 + 1,20 \times 10^{-3}\, x \end{array} \right\} \tag{2.68a}$$

$$v = 2,00 \times 10^{-5}\, x^3 - 6,10 \times 10^{-4}\, x^2 - 3,00 \times 10^{-5}\, x \tag{2.68b}$$

$$\boldsymbol{\sigma_x} = \left\{ \begin{array}{c} 0 \\ -1,20 \times 10^{1}\, x + 1,20 \times 10^{2} \end{array} \right\} \tag{2.68c}$$

$$\tau = -1,50 \times 10^{0} \tag{2.68d}$$

To have a qualitative check up of the goodness of the solution obtained we plot in figure 2.1 the cantilever transversal displacements $v(x)$.

2.3.4 Warping beam

In the previous section we highlight how HR principle permits to obtain the Timoshenko beam equations without introducing any shear factor, to this purpose we use a parabolic shear distribution. Really, this hypothesis does not agree with the hypotheses around displacements, in fact looking at τ local definition

$$\tau_{xy} = G\left(\frac{\partial}{\partial x}s_v(x, y) + \frac{\partial}{\partial y}s_u(x, y)\right) \tag{2.69}$$

it is possible to see that parabolic shear is congruent with y-cubic horizontal displacements.
To create a more correct model now we are going to consider this kind of displacements in the section, watching at the physical problem, this means that we are removing the hypothesis of plane sections and we let the section free to warp over its undeformed plane.

Hypotheses

About material, geometry and boundary conditions we maintain the same hypotheses used in the previous subsection.

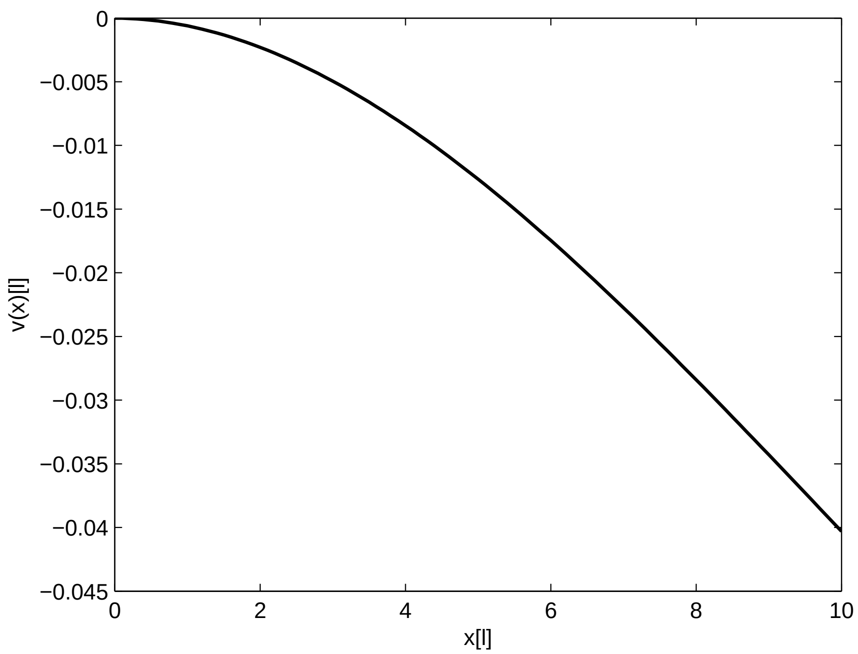

Figure 2.1: Transversal displacements of the cantilever for which we find the Timoshenko/Jourawsky solution

About the field we make the follow assumptions:

$$\boldsymbol{p_u} = \boldsymbol{p_\sigma} = \left\{ \begin{array}{c} 1 \\ y \\ y^2 \\ y^3 \end{array} \right\} \qquad \boldsymbol{p_\tau} = \left\{ \begin{array}{c} \frac{1}{2} - y \\ 1 - 4y^2 \\ \frac{1}{2} + y \end{array} \right\} \tag{2.70a}$$

$$\boldsymbol{p_v} = \{1\} \tag{2.70b}$$

About the choice of $\boldsymbol{p_\tau}$ here we do not satisfy in strong way the lateral surface equilibrium but, at the same time, we assume a field base that permits to satisfy it in a very easy way. In fact to impose conditions (2.43b) and (2.43c) it is sufficient to annul the first and the last terms of vector $\boldsymbol{\tau}$ and the first and the last lines or/and columns of the system matrices.

Governing equations

We proceed as we do in the previous subsection: we start evaluating the matrix terms. Since the complexity of integrals this procedure was implemented in a numerical algorithm. Then we solve the ODE system, the solution we obtain is the following:

$$\boldsymbol{u} = \begin{Bmatrix} u_1 \\ u_2 \\ u_3 \\ u_4 \end{Bmatrix} = \begin{Bmatrix} 0 \\ -6,00 \times 10^{-5}\,x^2 + 1,20 \times 10^{-3}\,x \\ 0 \\ 1,89 \times 10^{-13}\,x^2 - 3,78 \times 10^{-12}\,x \end{Bmatrix} \tag{2.71a}$$

$$v = 2,00 \times 10^{-5}\,x^3 - 6,10 \times 10^{-4}\,x^2 - 3,00 \times 10^{-5}\,x \tag{2.71b}$$

$$\boldsymbol{\sigma_x} = \begin{Bmatrix} \sigma_1 \\ \sigma_2 \\ \sigma_3 \\ \sigma_4 \end{Bmatrix} = \begin{Bmatrix} 0 \\ -1,20 \times 10^{1}\,x + 1,20 \times 10^{2} \\ 0 \\ 3,78 \times 10^{-8}\,x - 3,78 \times 10^{-7} \end{Bmatrix} \tag{2.71c}$$

$$\boldsymbol{\tau} = \begin{Bmatrix} \tau_1 \\ \tau_2 \\ \tau_3 \end{Bmatrix} \begin{Bmatrix} 0 \\ -1,50 \times 10^{0} \\ 0 \end{Bmatrix} \tag{2.71d}$$

$$\tag{2.71e}$$

In figures 2.2, 2.3, 2.4, 2.5 and 2.6 we represent the plots of most significant quantities.

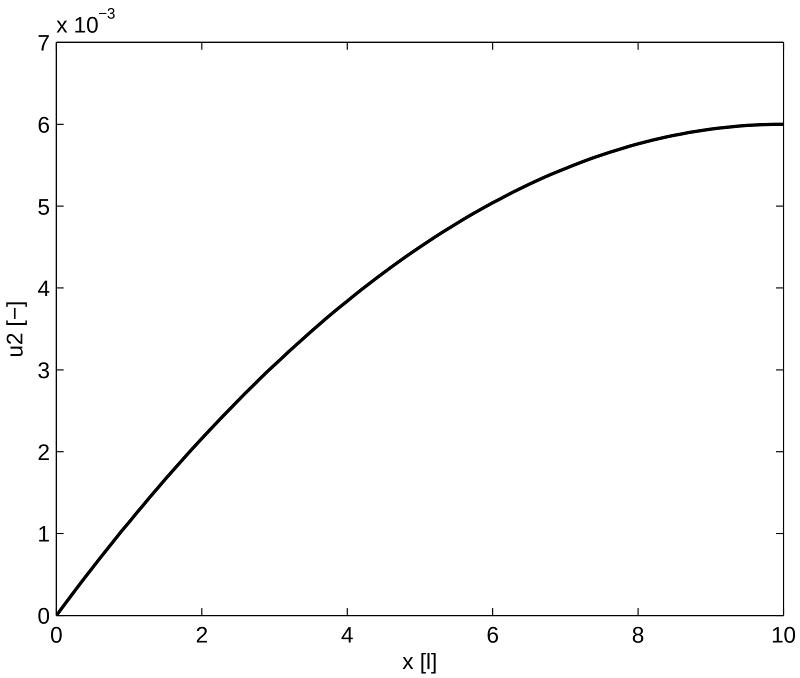

Figure 2.2: Rotation magnitude of the warping beam solution

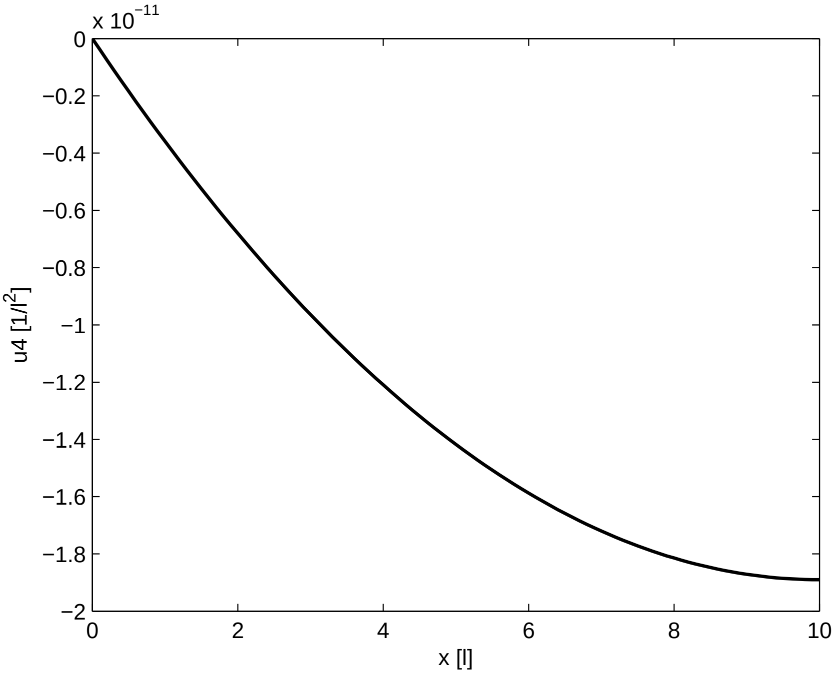

Figure 2.3: Warping magnitude of the warping beam solution

2.3.5 Discussion of results

The solid for which we are evaluating the solution satisfies clearly the Euler-Bernoulli hypotheses so, if the models are good, we expect equality between them.

First of all it is easy to see that in TJ beam solution the derivatives of v is the opposite of u_2 less a constant term 3×1^{-5}, so we can confirm that $\gamma = v' + u_2 = 3 \times 1^{-5} \approx 0$ as we expect, this confirm that, under the hypotheses we are working, the hypothesis to neglect γ is correct.

In the warping model orders of magnitude are crucial: u_4 is negligible respecting u_2 (they differ of 8 order of magnitude). This is a good behavior of the beam and confirm the goodness of TJ model under the hypotheses we are using. At the same time this statement indicate the consistency of the warping beam that converge to TJ model.
An other important aspect is that the displacements u_1 and u_3 are null:

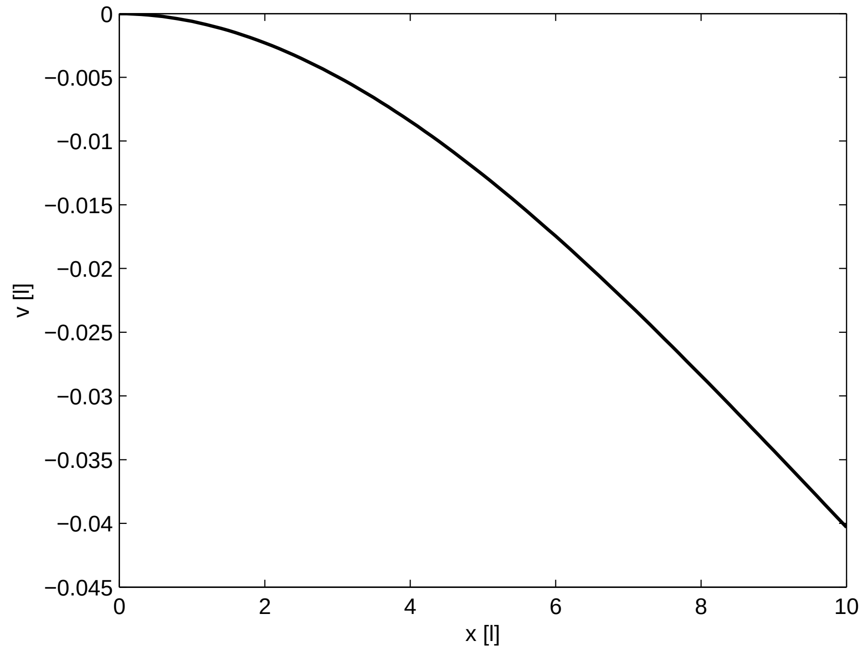

Figure 2.4: Transversal displacements of the warping beam solution

since the nature of loads we expect $u_1 = 0$ meanwhile we hope that $u_3 = 0$ because the strains related to it violate the lateral boundary conditions [2].

Assuming as control parameter the transversal free extreme displacement and the resultant stress in the clamp we report in table 2.1 the values of these quantities for the different models we develop and the relative errors assuming Euler-Bernoulli as exact solution.
It is possible to see how the models we developed are good: the maximum

beam model	$v(l)$	$\frac{v(l)}{v(l)}$	N(0)	M(0)	T(0)
Euler-Bernoulli	4.000×10^{-2}	1.0000	0.000	-10.000	1.000
Timoshenko	4.030×10^{-2}	1.0075	0.000	-10.000	1.000
warping beam	4.030×10^{-2}	1.0075	0.000	-10.000	1.000

Table 2.1: Extreme displacements and stresses using different beam models

transversal displacement difference between the models is less than the 1%. Again we can say that there is not substantial difference between the TJ and

[2]The statement that u_3 related stress violate the lateral equilibrium induces many authors to do not consider this degree of freedom in their work, as happened in [9]

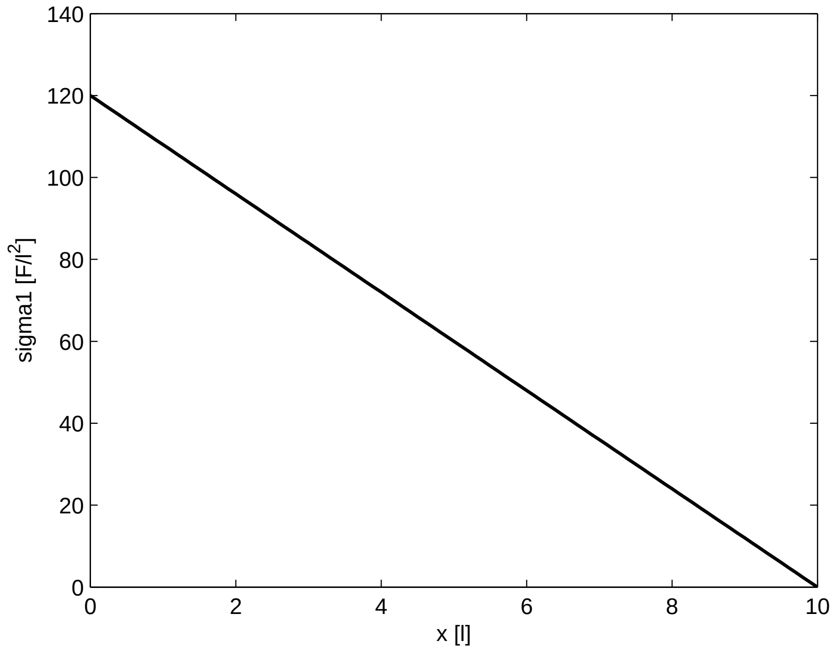

Figure 2.5: y-linear axial stress magnitude of the warping beam solution

the warping beams, that at last are the more correct model.
This few conclusions permit us to say that the models we have developed are good.

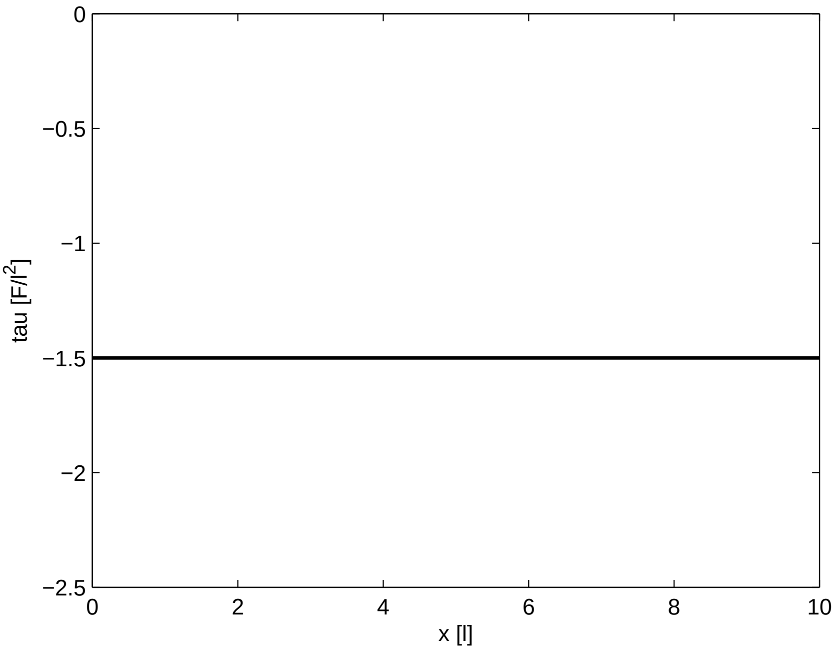

Figure 2.6: Shear magnitude of the warping beam solution

Chapter 3

Laminated beam

In this chapter we will discuss the model of a laminated beam. To build the model we will start from the homogeneous beam developed in section 2.3.4 because, as we have seen in the examples, the HR functional guarantees the best behavior of the models and warping beam kinematics is the most correct and complete one among those of the models previously discussed.
The first section is aimed to the description of the beam geometry and the discussion of base functions; in the next sections we will make some numerical examples and discuss the results obtained.

3.1 Hypotheses

3.1.1 Geometry

In chapter 1 we have presented a general beam geometry without better specifying the fields. In section 2.1 we assumed an homogeneous beam and smooth fields while now our purpose is to remove these assumptions. As for the geometry we assume a section as illustrated in figure 3.1, where a 3 layer beam section is represented while, obviously, in the model that we are going to develop we want to consider a n-layer beam. To describe the geometry and the properties of the beam we are working on, it is sufficient to define a vector $\boldsymbol{Y}$ that contains the layers geometry and an array $\boldsymbol{M}$ that give the mechanical properties of layers, they can be written as:

$$\boldsymbol{Y} = \left\{ \begin{array}{c} y_1 \\ y_2 \\ \vdots \\ y_n \\ y_{n+1} \end{array} \right\} \qquad \boldsymbol{M} = \left\{ \begin{array}{cc} E_1 & G_1 \\ E_2 & G_2 \\ \vdots & \vdots \\ E_n & G_n \end{array} \right\} \tag{3.1}$$

in which y_i and y_{i+1} are respectively the lower and the upper limits of the i^{th} layer and E_i and G_i are the mechanical properties of i^{th} layer.

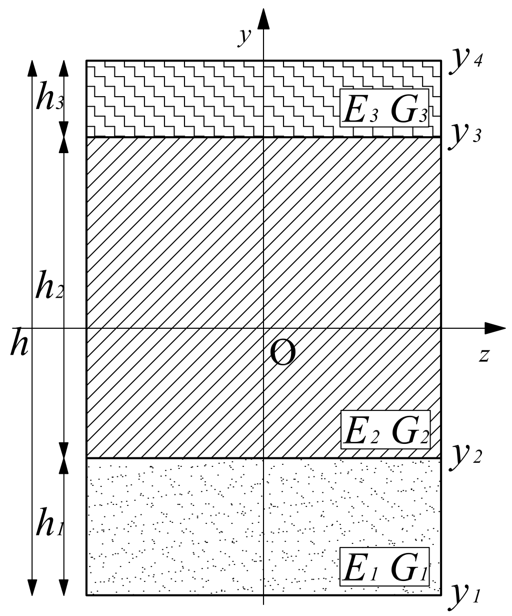

Figure 3.1: Section geometry and mechanical properties of a 3-layer beam

3.1.2 Field approximations

The choice of field approximation is the critical step in model development. In section 2.3.4 we developed a beam in which equilibrium and compatibility on its lateral surface can be very easily imposed. On this basis, in order to generate a laminated beam, we may applicate the homogeneous one to every layer constituting the beam and impose equilibrium and compatibility among them.
Therefore we are going to choose a field basis that is piecewise defined, smooth inside layers and that satisfies interlayer equilibrium and compatibility conditions. By these means, the model should bring the most accurate problem solution.

Developing the examples in section 2.3.3 we obtained the correct solution for TJ model. Indeed this happened only because in that model we forced the shape of shear distribution: in TJ we impose the shear to be parabolic even if it should be constant for compatibility. With more degrees of freedom, i.e. without forcing shear distribution, we expect it to tend to a displacement consistent distribution i.e. an homogeneous distribution. In this way we are sure to lose the exact solution. The only path that ensures a good behavior of the beam is to consider the warping model locally.
This choice implies high number of degrees of freedom: this may cause some problems and may reduce the efficiency of the model. We hope, in the definition of numerical model, to reduce the total number of degrees of freedom

with static condensations.

As a consequence of what we have just said, horizontal displacements must be locally cubic and globally continuous. In figure 3.2 we represent the base displacements for the three layers beam. In the same figure a possible shape

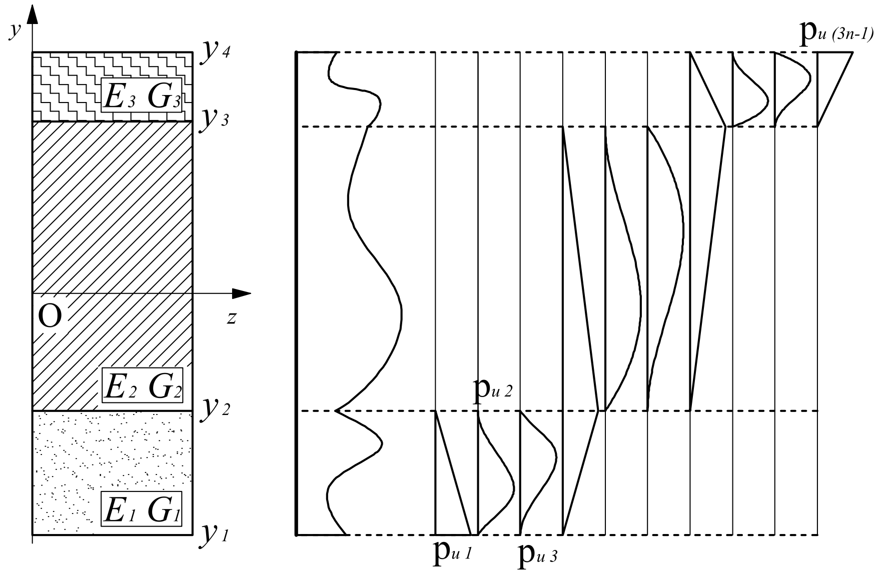

Figure 3.2: Horizontal displacement base

of resultant displacements is represented. This image highlights that the horizontal displacements $s_u \in C_0(A)$: this condition ensure us the compatibility is verified on the inter-layer surfaces. The analytical expression of the base functions on the i^{th} layer is reported in the following:

$$\boldsymbol{p_{ui}} = \left\{ \begin{array}{c} \dfrac{y_{i+1} - y}{y_{i+1} - y_i} \\ \dfrac{27}{4}\dfrac{y^3 + (2y_{i+1} - y_i)\, y^2 + \left(y_{i+1}^2 - 2y_{i+1}y_i\right) y - y_{i+1}^2 y_i}{(y_{i+1} - y_i)^3} \\ \dfrac{27}{4}\dfrac{y^3 - (2y_i + y_{i+1})\, y^2 + \left(y_i^2 + 2y_i y_{i+1}\right) y - y_i^2 y_{i+1}}{(y_{i+1} - y_i)^3} \\ \dfrac{y - y_i}{y_{i+1} - y_i} \end{array} \right\} \tag{3.2}$$

We assume that transversal displacements are constant on the section, so the base for this field is simply $p_v = \{1\}$.

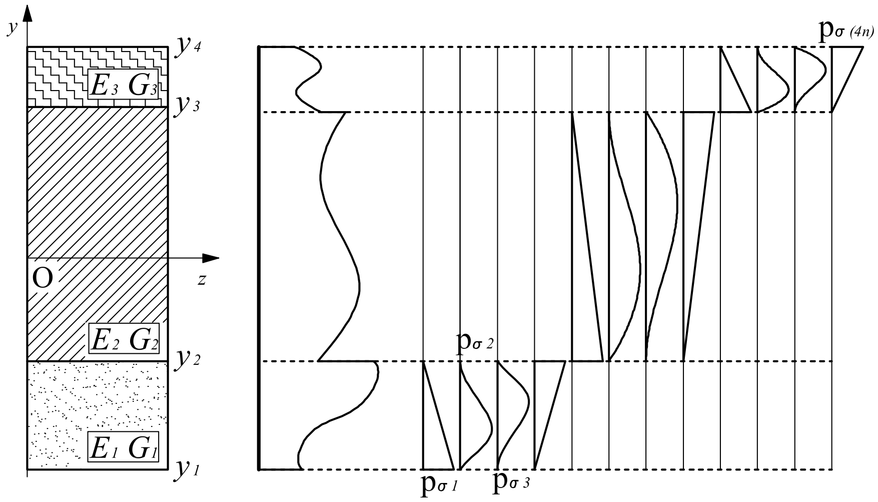

Figure 3.3: Base field of axial stress

Axial stress base is represented in figure 3.3. The local analytical expression of $\boldsymbol{p_{\sigma i}}$ base is the same of $\boldsymbol{p_{ui}}$. As it is showed in figure, these two fields differ only by inter-layer continuities: axial stress can be discontinuous.

The base of shear distribution is represented in figure 3.4. The possible shear distribution represented in the same figure shows that $\tau \in C_0(A)$. This assumption ensure us that the inter-layer surface equilibrium is satisfied.
The analytical expression of τ base is reported in the following:

$$\boldsymbol{p_{\tau}} = \left\{ \begin{array}{c} \dfrac{y_{i+1} - y}{y_{i+1} - y_i} \\ 4\dfrac{-y^2 + (y_{i+1} + y_i)\,y - y_{i+1}y_i}{(y_{i+1} - y_i)^2} \\ \dfrac{y - y_i}{y_{i+1} - y_i} \end{array} \right\} \tag{3.3}$$

The choice of each local field component is mainly motivated by practical problems:

- It is easy to distinguish the linear components of the displacements from the warping components.
- It is easy to impose inter-layer compatibility and equilibrium: since the base functions are involved in computation of coefficient matrices

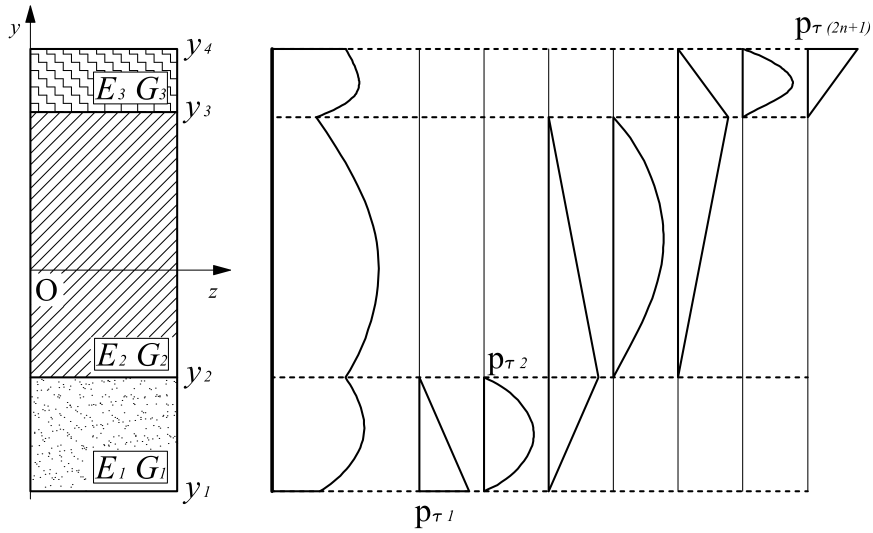

Figure 3.4: Base field of shear stress

it is possible to evaluate coefficients in every layer and assemble the global matrices with an assembling procedure analogous analogous to that used in FEM algorithm.

- The scatter plots of global matrices are good: the whole of matrices are multi - diagonal: this fact is useful for the numerical evaluation of the problem solution.

3.2 Trivial example

First of all we will consider a trivial example: we assume a section composed by more layers, all of which with the same mechanical characteristics. We are hence working on the homogeneous beam: in this case we are going to use more complex field basis to obtain once again the solution of the warping model.

3.2.1 Geometry, materials and boundary conditions

As for the global dimensions and the characteristics of materials we will use the same parameters we already defined in 2.3.3.

In addition to what we already know we must define the layer geometry:

$$\boldsymbol{Y} = \begin{Bmatrix} -\frac{1}{2} \\ -\frac{1}{6} \\ \frac{1}{2} \end{Bmatrix} \tag{3.4}$$

This choice arises by an arbitrary assumption: we are simply adopting the lowest and most significant number of degrees of freedom. The position of discontinuity surface answers to the need of having not any symmetry in the model that could "help" a good behavior of the beam.

The governing equations of the problem are (2.36), (2.43) and (2.47).
As for the boundary conditions of the model we are working on a beam clamped at both extremes and without any load. We impose an unitarian transversal displacement to one of the two extremes, in particular $v(10) = 1$.

3.2.2 About the solution computation

The problem formulated in the previous section is very hard to solve: it is a ODE system of 21 unknowns in first order 21 ODEs. As explained in section 2.2.3, the problem can be reduced to a displacement formulation: in this case the problem is a ODE system of 8 unknowns in 8 second order ODEs.
The two possible formulations highlight a problem: watching the first one we expect to obtain a 21-parameter dependent solution, on the opposite looking at the second formulation we can see that the solution depends only on 16 parameters. Since the physical problem is the same we expect to obtain the same solution and so the same number of parameters, independently on the formulation.
Being p the number of unknown displacements and q the unknown stress one, we can see, watching the boundary conditions (2.43) and (2.47), that the first imposes p conditions on q stresses and the second imposes q conditions on p displacements.
In the case we are discussing, in which $p = 8$ and $q = 13$, equation (2.43) imposes 8 significant conditions on 13 variables while equation (2.47) imposes 13 conditions. Since there are only 8 variables, the significant conditions can be at most 8. So globally the significant conditions we can impose are 16 in every case [1].

To solve the ODE system we used the programme *Maple 11* that permits to

[1] The stress-displacement formulation has a good behavior if $p = q$. This always happened in examples of section 2.1 in which we used this formulation without having this kind of problems

obtain the analytical solution with symbolic calculus. Unfortunately, due to problem complexity and program limits, we did not obtain do not lead to obtain a completely exhaustive solution:

- it was possible to calculate the analytical solution for both problem formulations only without imposition of boundary conditions;
- when they were imposed it was necessary to use a numerical algorithm and the displacement formulation to evaluate the solution ;
- when we are using the displacement formulation the program does not allow to impose Robin boundary conditions, so it is not possible to bound with a force the beam extremities .

This last statement led us to impose the boundary conditions illustrated at the beginning of this section.

3.2.3 Results

Analytical solution

The analytical solution of the problem is very complex and we do not report it here. However we can make some interesting remarks on it.

- The solution of stress and displacement formulation depends on only 16 parameters. This statement corroborates the fact that the problem really depends only on 16 parameters, as discussed in the previous section.
- The structure of the solution is the following:

$$\Phi = C_i e^{\pm \alpha x} + C_j x^n \tag{3.5}$$

  i.e. the solution contains exponential terms and polynomial terms, the latter give the first-order beam solution, while the former, being significantly different from zero only near the extremities, could model the extinction of local effects produced by the shape of external loads. Nevertheless this good and unexpected behavior of the solution must be considered carefully in fact it can not be used to evaluate local stress magnitudes because in the 3D solution there is significant transversal axial stress $\sigma_y \neq 0$, while we are assuming it to be always null.

- The degree of solution polynomials is the same of the one of TJ or warping models.
- Structure of $\boldsymbol{\tau}$ variable is the following: $\tau_i = C\beta_i$ where C is the same in every vector term, depending on the boundary conditions of problem, while β_i depends on the component. This means that C gives the

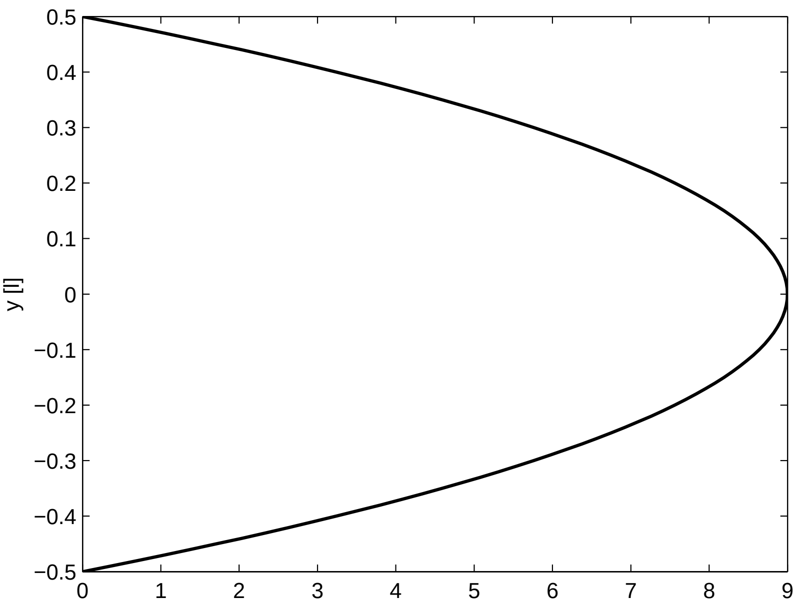

Figure 3.5: Generic shear field shape for a 2-layer beam

magnitude of the resultant shear and $\beta_i \cdot p_{\tau i}$ gives the shape of the shear field. In figure 3.5 we report a plot of the field as obtained by the analytical solution: it is evident that the shape of resultant shear is parabolic.

Thanks to these considerations we may say that the model consider so far can show a good behavior.

Numerical solution

Now we will discuss the most significant results obtained by means of the numerical algorithm. First of all we report, in figure 3.6, the plot of transversal displacement. Qualitatively, it is possible to see that the solution is exact and reflects what we were expecting.
In figures 3.7 and 3.9 we report horizontal displacement field and shear field on the section at $x = 5$ respectively. In the same plots we can compare the multi-layered model solution and the warping beam one. In figures 3.8 and 3.10 we report the plots of the relative errors, evaluated as $\Phi_{2lay} - \Phi_{warp}$.
Qualitatively the solution obtained is exact. Evaluating more accurately the error, we can make some remarks.

- The errors are always of 2 or 3 orders of magnitude inferior than the magnitude of the variables they are related to. This means that the

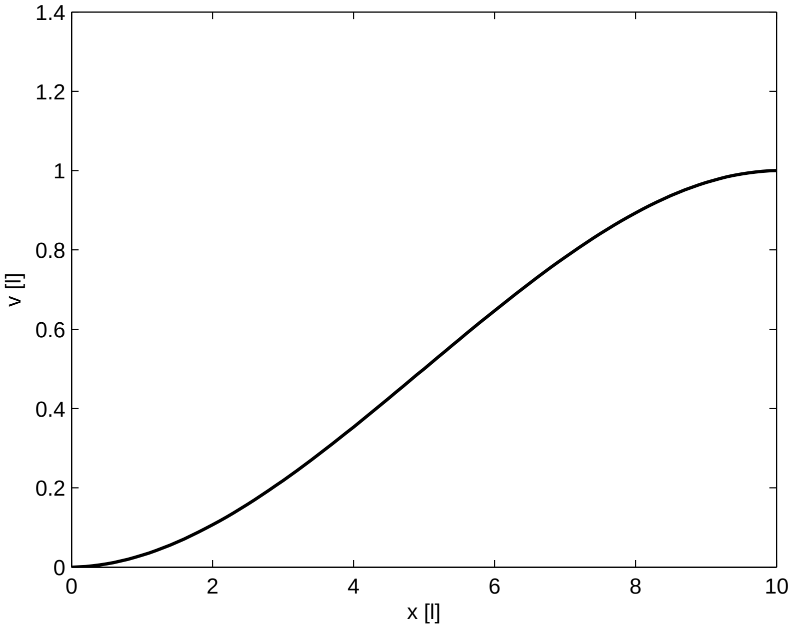

Figure 3.6: 2-layer beam transversal displacements, numerical result

relative error is always less than 1 %. Relative shear error is generally less than relative displacement error.

- The displacement error has the same order of magnitude as the warping variable on the section. We can try to justify this behavior realizing that also y-linear error has the same magnitude, so we can make the hypothesis that in multi-layer beam the warping variables could compensate the error of y linear variables.

- The mean value of error on the section is null [2], in other words:

$$\int_A (s_{u2lay} - s_{uwarp})\, dA = -2,54 \times 10^{-12} \approx 0. \tag{3.6}$$

  This statement corroborate the previous hypothesis about the behavior of warping.

- The warping error, obtained as difference between the global error and the linear error is bigger inside the beam thickness, where also shear error is big, and it tends to become smaller near the lateral surfaces, where shear error is null. This lead us to think that the warping error and the shear error are in some way related the one to the other.

[2] As for the value of this integral it worths noting that 10^{-11} is the error tolerance of numerical algorithm.

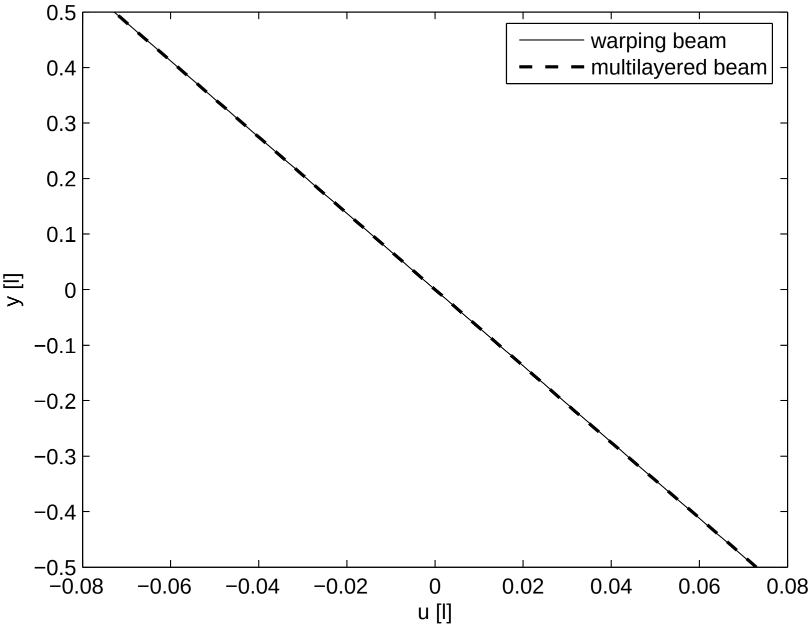

Figure 3.7: 2-layer beam horizontal displacements evaluated at x=5, numerical result

In table 3.1 we report numeric values of axial stress, bending moment and shear stress resultants in the origin section and their relative errors, assuming as the exact model the Euler-Bernoulli beam and the transversal displacement at $x = 2,5$ with its the relative error[3]. Hence it is worth making the following remarks.

- The axial resultant force is always correctly predicted. In 2-layer beam error must be imputed to the numerical method too.
- There are not significant differences between TJ, warping and the 2-layer models. It is possible to notice a small difference between the latter and the former two but this can be attributed, once again, to the numerical error.
- There is a significant difference (2 or 3 %) between the Euler-Bernoulli solution and the others: particularly it is possible to see that the Euler-Bernoulli beam is more rigid than the others: in the EB solution we have stronger forces and less strains. We could have expected this result: having less degrees of freedom the EB beam has more inter-

[3] The number “1” representing axial force errors means that the solution is exact, differently it is not possible to evaluate the error

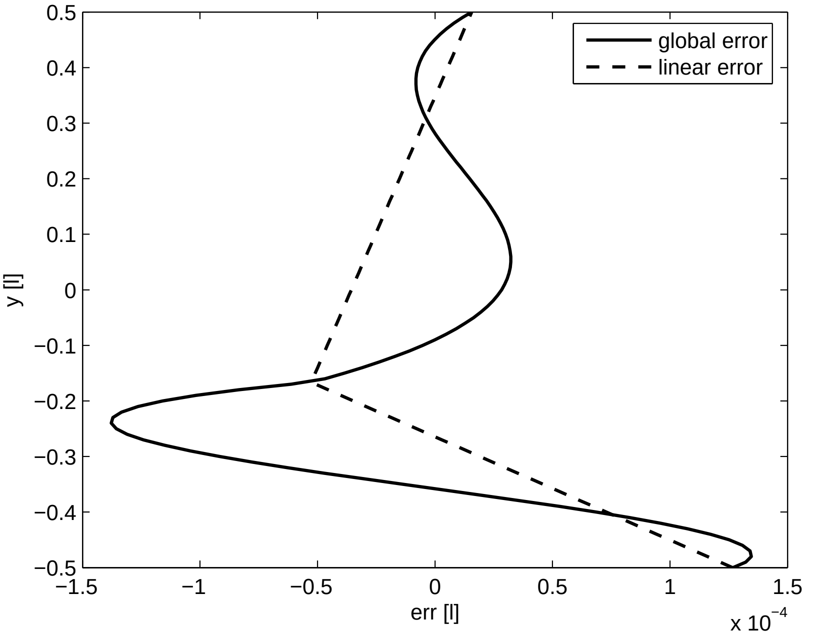

Figure 3.8: 2-layer beam horizontal displacement error evaluated at x=5

nal constraints and this justifies the increment of stiffness. This phenomenon is offen mentioned in literature.

- The statement that EB beam is more rigid could be deduced also watching table 2.1. However in this table it is not possible to see differences of the forces because the cantilever is an isostatic structure and so the reactions depend only on external force; in the opposite case the model we are considering is now hyper-static and the external reactions are also influenced by beam.

We analyzed also an homogeneous beam composed by 3 layers. Once more, we obtained the same results already illustrated.

3.2.4 Extinction of local effects

As we have already discussed in section 3.2.2 the model we developed can predict the extinction of local effects produced by the shape of external loads and displacements. In fact we know that, far from the boundary, the behavior of the elastic solid depends only on the resultant of external loads or average displacements. Moreover the theory ensures that the local effects are significant only in a region equal to $1 \div 1.5\tilde{h}$ in which $\tilde{h}$ is the characteristic dimension of the beam section.

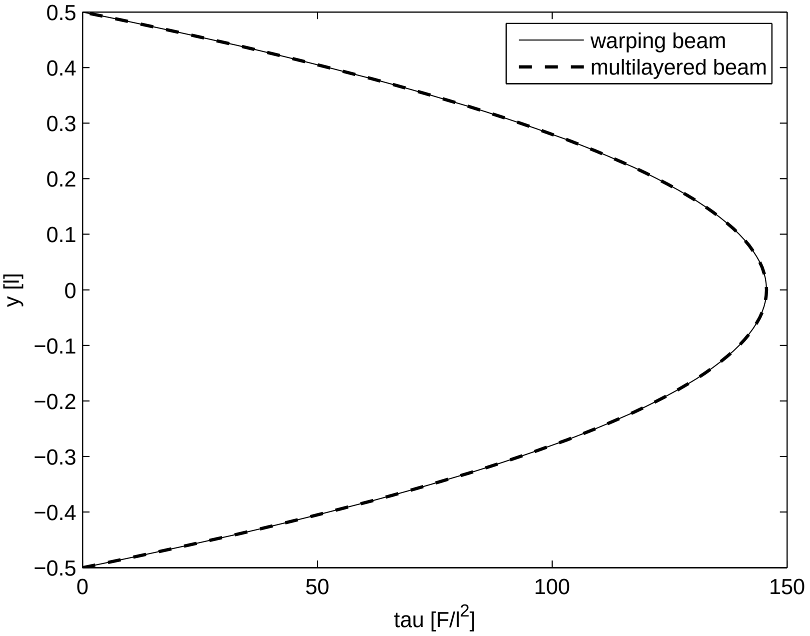

Figure 3.9: 2-layer beam shear distribution evaluated at x=5, numerical result

Now we will impose a "not homogeneous"[4] boundary condition that will produce local effects. Afterward, we will study how the model answers to this imposition. On the boundary, we assign null displacements everywhere except for the first degree of freedom of s_u in the origin, which we impose to be equal to 1 ($u_1(0) = 1$).

In the following we will plot displacements and stress distributions near the extreme in which we imposed the not homogeneous displacement. The horizontal displacements at x=0 in figure 3.12 are the plot of the imposed boundary conditions.

- Watching figure 3.11 it is possible to see how the global effect of our boundary condition is simply the imposition of a non null average rotation in the origin.
- Looking at figure 3.13 we realize that the shear is the field that extinguishes the local effects less quickly than the others. It worths remarking that this field at $x = 1.5\tilde{h}$ is not parabolic but the maximum

[4]by this term we define every boundary condition that is able to produce significant local effects, in other words every distribution of forces or displacements different from what we can impose on homogeneous beam

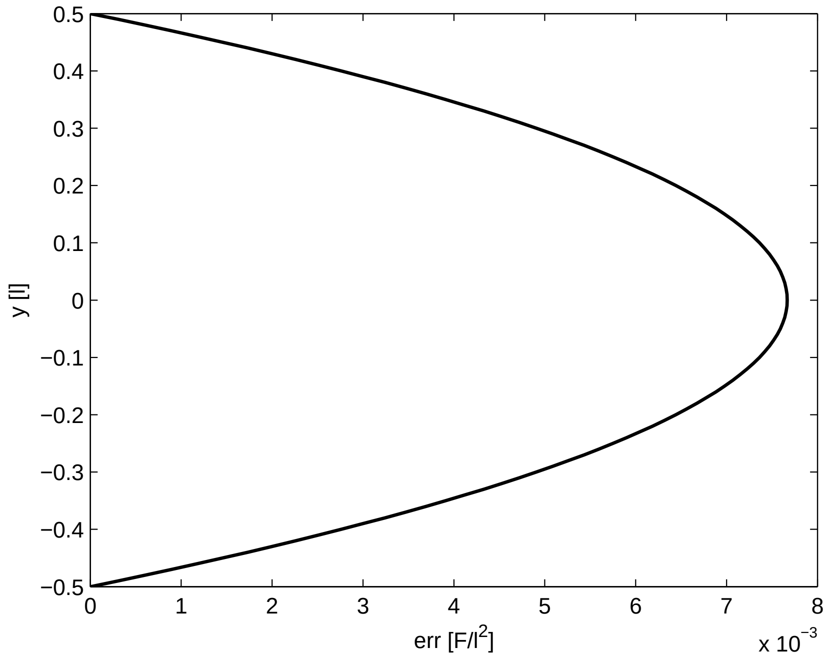

Figure 3.10: 2-layer beam shear error evaluated at x=5

shear on the section has the same order of magnitude of the exact distribution. So the statement we previously inferred about the length of extinction region can be considered true in this case too.

- Being the boundary condition not symmetric we expected, as global effect, a non symmetric behavior of the section: in fact, as it is possible to see in figure 3.14 the neutral axis of the section is not at the half of its height.

This behavior of the beam can obviously be considered (or not) in numerical models using (or not) adequate shape functions. Nevertheless it can be interesting to use the displayed behavior to model some problems of interest in appliance of beam theory such as:

- Section geometry discontinuities.
- Plastic hinges model.
- Every kind of problem in which local effect could be significant.

beam model	$v(2.5)$	$\frac{v}{v_{EB}}$	$T(0)$	$\frac{T}{T_{EB}}$
Euler-Bernoulli	$1,5625 \times 10^{-1}$	1.0000	-1.0000×10^{2}	1.0000
Timoshenko	1.5898×10^{-1}	1.0175	-9.7087×10^{1}	0.9709
warping beam	1.5898×10^{-1}	1.0175	-9.7087×10^{1}	0.9709
2-layer beam	1.5896×10^{-1}	1.0173	-9.7092×10^{1}	0.9709
beam model	$N(0)$	$\frac{N}{N_{EB}}$	$M(0)$	$\frac{M}{M_{EB}}$
Euler-Bernoulli	0.0000×10^{-7}	1.0000	5.0000×10^{2}	1.0000
Timoshenko	0.0000×10^{-7}	1.0000	4.8544×10^{2}	0.9709
warping beam	0.0000×10^{-7}	1.0000	4.8544×10^{2}	0.9709
2-layer beam	-1.6140×10^{-7}	-	4.8546×10^{2}	0.9709

Table 3.1: Stress resultants and displacements at significant sections

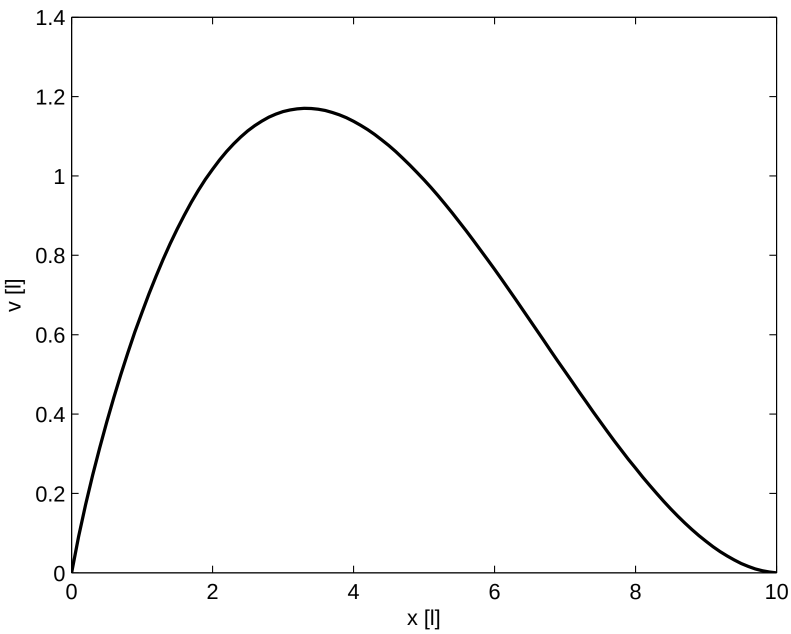

Figure 3.11: Transversal displacements obtained as solution of the problem with not homogeneous boundary conditions

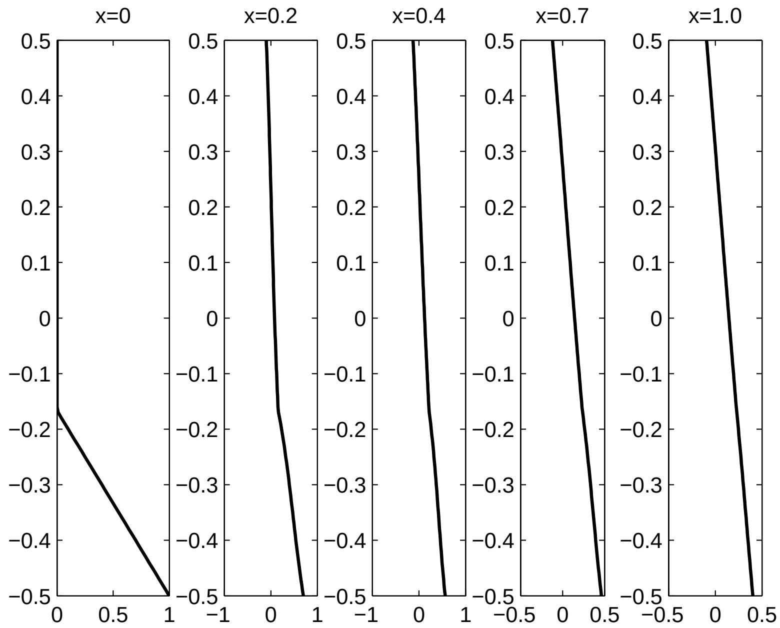

Figure 3.12: Section displacements near the section in which we apply not homogeneous boundary condition

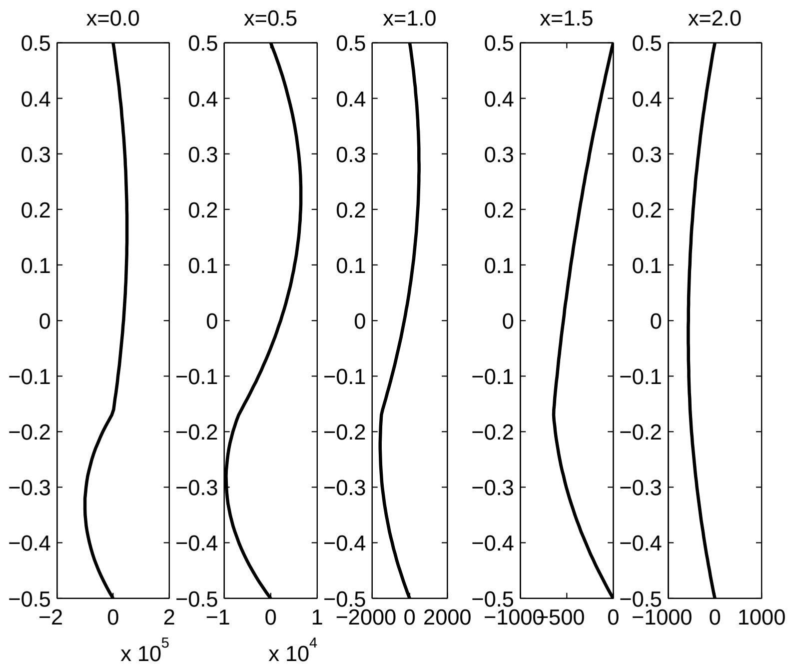

Figure 3.13: Shear distributions near the section in which we apply not homogeneous boundary condition

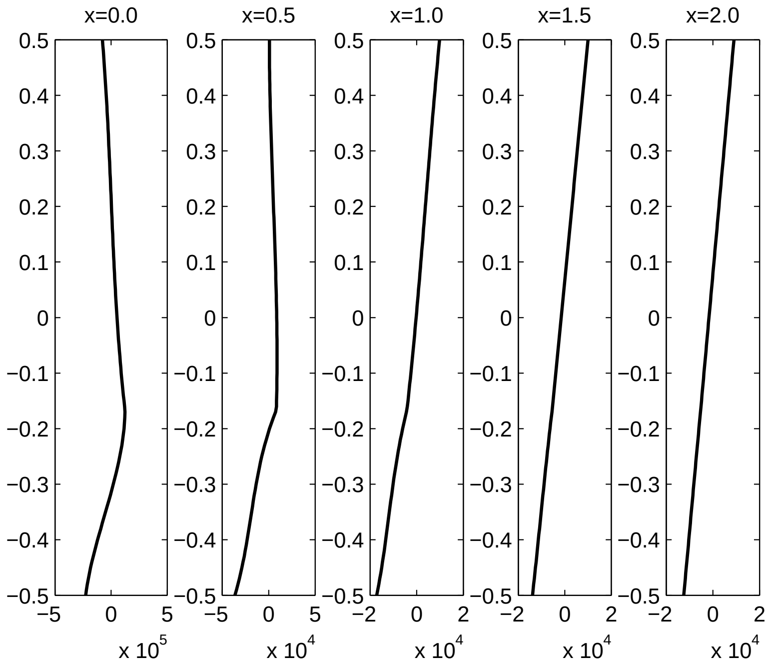

Figure 3.14: Axial stress near the section in which we apply not homogeneous boundary condition

3.3 Advanced example

3.3.1 Geometry and materials

For the advanced example we define the following geometry and material vectors:

$$\boldsymbol{Y} = \left\{ \begin{array}{c} -0.5 \\ -0.3 \\ 0.3 \\ 0.5 \end{array} \right\} \qquad \boldsymbol{M} = \left\{ \begin{array}{cc} 1.00 \times 10^5 & 4.00 \times 10^4 \\ 2.40 \times 10^4 & 1.00 \times 10^4 \\ 1.00 \times 10^5 & 4.00 \times 10^4 \end{array} \right\} \tag{3.7a}$$

The beam is composed by 3 layers the intermediate of which has mechanical properties poorer than the others.
We choose a symmetric section and we expect consequently to obtain symmetric or emi-symmetric fields on the section.

As a boundary condition we impose null displacements everywhere except for an unitarian transversal displacement at $x = 10$.

3.3.2 Results

Here we are going to report the plots of most significant quantities obtained by the solution of the problem we have just defined. It is interesting to note that in figure 3.15 the horizontal displacements are nearly linear respect to y.
Moreover it is possible to see that, as we expected, the solutions we obtained are all odd or even respect y domine.

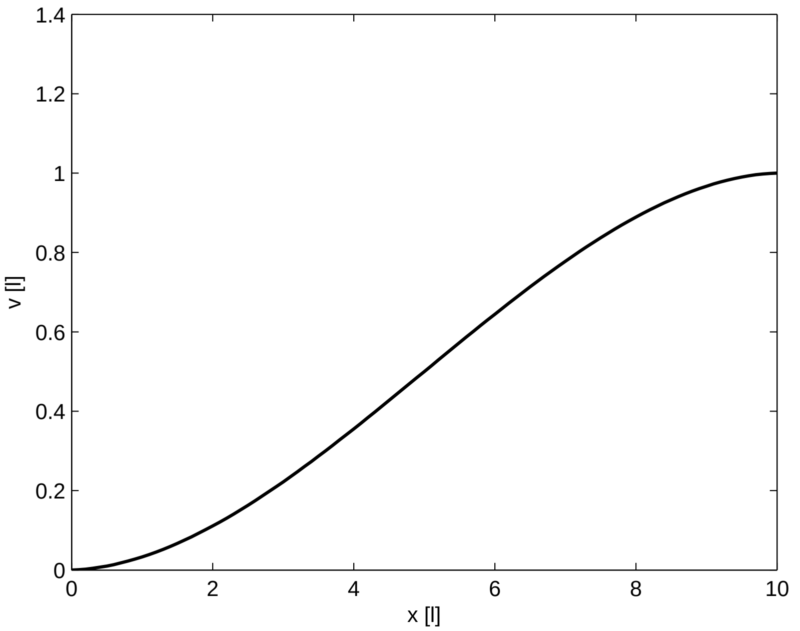

Figure 3.15: Transversal displacements obtained as solution of the non homogeneous beam

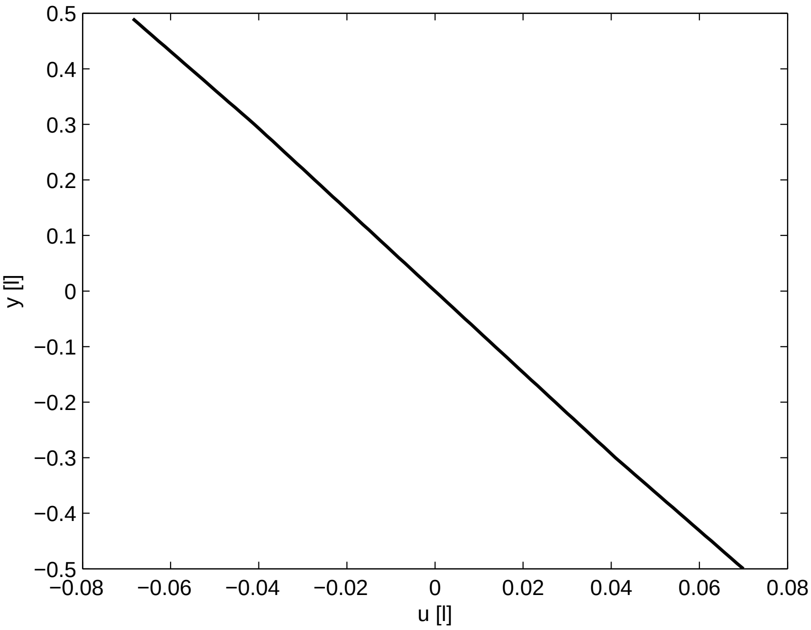

Figure 3.16: Horizontal displacements on the section at the half of the beam

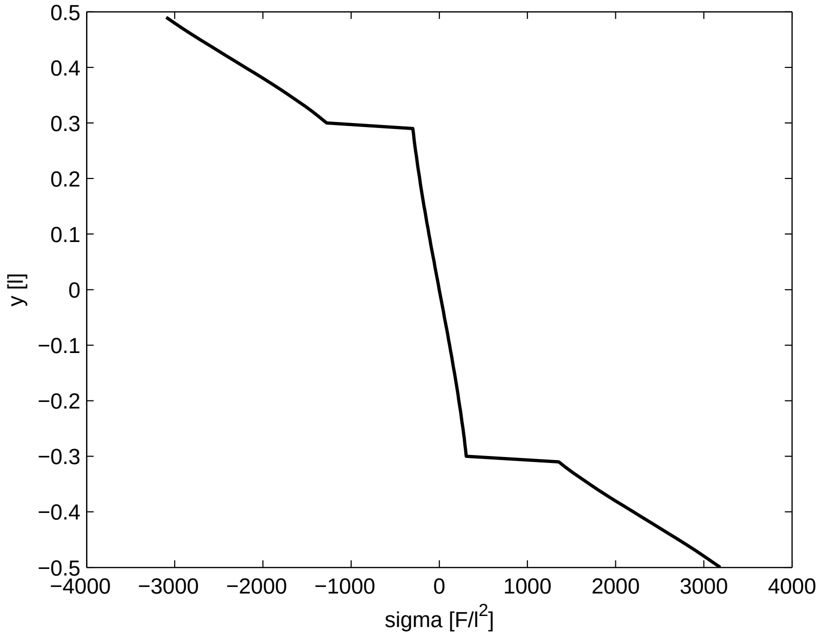

Figure 3.17: Axial stress distribution at x=0.00

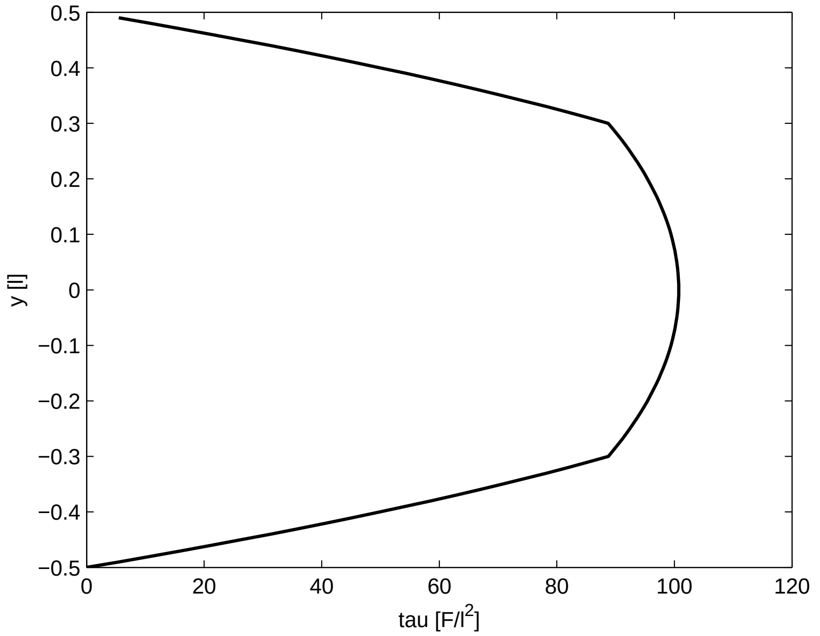

Figure 3.18: Shear distribution at x=0.00

Chapter 4

The numerical beam model

In this chapter we will develop the numerical model of the laminated beam we have previously analyzed.
We will start by developing the weak formulation of the problem, introducing field hypotheses and reducing the problem to an algebraic form. Then we will go on discussing the choice of the so called shape functions and, at last, we will make some examples and discuss them.

4.1 Weak formulation

In order to develop the numerical method we must start from a weak formulation of the problem. The most natural choice is to start from the stationarity of the functional from which we derivated the governing equations.
In section 1.3.3 we wrote two possible weak formulations: the first is equation (1.12), and the second is equation (1.14). Usually people prefer to develop numerical models starting from the first of the two formulations, that is properly the stationarity of functional and lead to a symmetric formulation. This is the path we want to use.

So starting form equation (1.12), we rewrite it adopting notations and conventions of section 2.1. We obtain:

$$\delta J_{HR} = \int_{\Omega} \left(\boldsymbol{L}^T \delta \boldsymbol{s}\right)^T \boldsymbol{\sigma} \, d\Omega + \int_{\Omega} \delta \boldsymbol{\sigma}^T \boldsymbol{L}^T \boldsymbol{s} \, d\Omega - \tag{4.1a}$$

$$\int_{\Omega} \delta \boldsymbol{\sigma}^T \boldsymbol{D}^{-1} \boldsymbol{\sigma} \, d\Omega - \int_{\Omega} \delta \boldsymbol{s}^T \boldsymbol{f} \, d\Omega - \tag{4.1b}$$

$$\int_{\partial\Omega_t} \delta \boldsymbol{s}^T \boldsymbol{t} \, dS - \int_{\partial\Omega_s} \left(\delta \boldsymbol{\sigma} \boldsymbol{N}\right)^T \left(\boldsymbol{s} - \bar{\boldsymbol{s}}\right) \, dS - \int_{\partial\Omega_s} \delta \boldsymbol{s}^T \boldsymbol{N} \boldsymbol{\sigma} \, dS = 0 \tag{4.1c}$$

As we did in section 2.1 we split the weak formulation in body equation, bounded displacement surface and force boundary.

4.1.1 Body equations

Substituting definitions (2.2) and developing matrix products in terms (4.1a) and (4.1b) we obtain:

$$\int_\Omega \left[\boldsymbol{L}^T\delta\boldsymbol{s}\right]^T \boldsymbol{\sigma}\, d\Omega + \int_\Omega \delta\boldsymbol{\sigma}^T\boldsymbol{L}^T\boldsymbol{s}\, d\Omega - \tag{4.2a}$$

$$\int_\Omega \delta\boldsymbol{\sigma}^T\boldsymbol{D}^{-1}\boldsymbol{\sigma}\, d\Omega - \int_\Omega \delta\boldsymbol{s}^T\boldsymbol{f}\, d\Omega = 0 \tag{4.2b}$$

Introducing the field definitions (2.2) and developing the matrix product we arrive to the following formulation:

$$\int_\Omega [\delta\boldsymbol{u}'^T, \delta\boldsymbol{v}'^T] \left[\begin{array}{cc} \boldsymbol{p_u}\boldsymbol{p_\sigma}^T & \boldsymbol{0} \\ \boldsymbol{0} & \boldsymbol{p_v}\boldsymbol{p_\tau}^T \end{array}\right] \left\{\begin{array}{c} \boldsymbol{\sigma_x} \\ \boldsymbol{\tau} \end{array}\right\} + [\delta\boldsymbol{u}^T, \delta\boldsymbol{v}^T] \left[\begin{array}{cc} \boldsymbol{0} & \boldsymbol{p_u}'\boldsymbol{p_\tau}^T \\ \boldsymbol{0} & \boldsymbol{0} \end{array}\right] \left\{\begin{array}{c} \boldsymbol{\sigma_x} \\ \boldsymbol{\tau} \end{array}\right\} + \tag{4.3a}$$

$$[\delta\boldsymbol{\sigma_x}^T, \delta\boldsymbol{\tau}^T] \left[\begin{array}{cc} \boldsymbol{p_\sigma}\boldsymbol{p_u}^T & \boldsymbol{0} \\ \boldsymbol{0} & \boldsymbol{p_\tau}\boldsymbol{p_v}^T \end{array}\right] \left\{\begin{array}{c} \boldsymbol{u}' \\ \boldsymbol{v}' \end{array}\right\} + [\delta\boldsymbol{\sigma_x}^T, \delta\boldsymbol{\tau}^T] \left[\begin{array}{cc} \boldsymbol{0} & \boldsymbol{0} \\ \boldsymbol{p_\tau}\boldsymbol{p_u}'^T & \boldsymbol{0} \end{array}\right] \left\{\begin{array}{c} \boldsymbol{u} \\ \boldsymbol{v} \end{array}\right\} - \tag{4.3b}$$

$$[\delta\boldsymbol{\sigma_x}^T, \delta\boldsymbol{\tau}^T] \left[\begin{array}{cc} \dfrac{\boldsymbol{p_\sigma}\boldsymbol{p_\sigma}^T}{E} & \boldsymbol{0} \\ \boldsymbol{0} & \dfrac{\boldsymbol{p_\tau}\boldsymbol{p_v}^T}{G} \end{array}\right] \left\{\begin{array}{c} \boldsymbol{\sigma_x} \\ \boldsymbol{\tau} \end{array}\right\} - [\delta\boldsymbol{u}^T, \delta\boldsymbol{u}^T] \left\{\begin{array}{c} \boldsymbol{p_u} f_x \\ \boldsymbol{p_v} f_y \end{array}\right\} d\Omega = 0 \tag{4.3c}$$

As happened in section 2.1, only the terms inside the matrices depends on the sections variable, so it is possible to split the integrals. Using definitions (2.35) and introducing the following

$$\boldsymbol{P_{u'\tau}} = \int_A \boldsymbol{p}'_{\boldsymbol{u}}\boldsymbol{p_\tau} dA \tag{4.4}$$

we obtain:

$$\begin{aligned} \int_l [\delta\boldsymbol{u}'^T, \delta\boldsymbol{v}'^T] \left[\begin{array}{cc} \boldsymbol{P_{u\sigma}} & \boldsymbol{0} \\ \boldsymbol{0} & \boldsymbol{P_{v\tau}} \end{array}\right] \left\{\begin{array}{c} \boldsymbol{\sigma_x} \\ \boldsymbol{\tau} \end{array}\right\} + [\delta\boldsymbol{u}^T, \delta\boldsymbol{v}^T] \left[\begin{array}{cc} \boldsymbol{0} & \boldsymbol{P_{u'\tau}} \\ \boldsymbol{0} & \boldsymbol{0} \end{array}\right] \left\{\begin{array}{c} \boldsymbol{\sigma_x} \\ \boldsymbol{\tau} \end{array}\right\} + \\ [\delta\boldsymbol{\sigma_x}^T, \delta\boldsymbol{\tau}^T] \left[\begin{array}{cc} \boldsymbol{P_{\sigma u}} & \boldsymbol{0} \\ \boldsymbol{0} & \boldsymbol{P_{\tau v}} \end{array}\right] \left\{\begin{array}{c} \boldsymbol{u}' \\ \boldsymbol{v}' \end{array}\right\} + [\delta\boldsymbol{\sigma_x}^T, \delta\boldsymbol{\tau}^T] \left[\begin{array}{cc} \boldsymbol{0} & \boldsymbol{0} \\ \boldsymbol{P_{\tau u'}} & \boldsymbol{0} \end{array}\right] \left\{\begin{array}{c} \boldsymbol{u} \\ \boldsymbol{v} \end{array}\right\} - \\ [\delta\boldsymbol{\sigma_x}^T, \delta\boldsymbol{\tau}^T] \left[\begin{array}{cc} \boldsymbol{P_{\sigma\sigma}} & \boldsymbol{0} \\ \boldsymbol{0} & \boldsymbol{P_{\tau\tau}} \end{array}\right] \left\{\begin{array}{c} \boldsymbol{\sigma_x} \\ \boldsymbol{\tau} \end{array}\right\} - [\delta\boldsymbol{u}^T, \delta\boldsymbol{u}^T] \left\{\begin{array}{c} \boldsymbol{F_x} \\ \boldsymbol{F_y} \end{array}\right\} dx = 0 \end{aligned} \tag{4.5}$$

4.2 Field approximations and algebraic reduction

Now we must introduce the hypothesis of finite dimension of fields: we suppose that every unknown field can be expressed as a linear combination of the so called shape functions weighted with scalar quantities. In the following we introduce the new notation that uses the shape functions.

$$\boldsymbol{u}(x) \quad \Rightarrow \quad \boldsymbol{B}_u(x) \quad \hat{\boldsymbol{u}} \tag{4.6a}$$
$$\boldsymbol{v}(x) \quad \Rightarrow \quad \boldsymbol{B}_v(x) \quad \hat{\boldsymbol{v}} \tag{4.6b}$$
$$\boldsymbol{\sigma_x}(x) \quad \Rightarrow \quad \boldsymbol{B}_\sigma(x) \quad \hat{\boldsymbol{\sigma}} \tag{4.6c}$$
$$\boldsymbol{\tau}(x) \quad \Rightarrow \quad \boldsymbol{B}_\tau(x) \quad \hat{\boldsymbol{\tau}} \tag{4.6d}$$

The problem we are developing can be written as:

$$\begin{aligned}
&\int_l (\,\delta\hat{\boldsymbol{u}}^T\, \boldsymbol{B}_u'^T \boldsymbol{P_{u\sigma}} \boldsymbol{B}_\sigma\, \hat{\boldsymbol{\sigma}} + \delta\hat{\boldsymbol{v}}^T\, \boldsymbol{B}_v'^T \boldsymbol{P_{v\tau}} \boldsymbol{B}_\tau\, \hat{\boldsymbol{\tau}} + \\
&\quad \delta\hat{\boldsymbol{u}}^T\, \boldsymbol{B}_u^T \boldsymbol{P_{u'\tau}} \boldsymbol{B}_\tau\, \hat{\boldsymbol{\tau}} + \delta\hat{\boldsymbol{\sigma}}^T\, \boldsymbol{B}_\sigma^T \boldsymbol{P_{\sigma u}} \boldsymbol{B}_u'\, \hat{\boldsymbol{u}} + \\
&\quad \delta\hat{\boldsymbol{\tau}}^T\, \boldsymbol{B}_\tau^T \boldsymbol{P_{\tau v}} \boldsymbol{B}_v'\, \hat{\boldsymbol{v}} + \delta\hat{\boldsymbol{\tau}}^T\, \boldsymbol{B}_\tau^T \boldsymbol{P_{\tau u'}} \boldsymbol{B}_u\, \hat{\boldsymbol{u}} - \\
&\quad \delta\hat{\boldsymbol{\sigma}}^T\, \boldsymbol{B}_\sigma^T \boldsymbol{P_{\sigma\sigma}} \boldsymbol{B}_\sigma\, \hat{\boldsymbol{\sigma}} - \delta\hat{\boldsymbol{\tau}}^T\, \boldsymbol{B}_\tau^T \boldsymbol{P_{\tau\tau}} \boldsymbol{B}_\tau\, \hat{\boldsymbol{\tau}}\ )\, dx = \\
&\int_l (\delta\hat{\boldsymbol{u}}^T\, \boldsymbol{B}_u\, F_u + \delta\hat{\boldsymbol{v}}^T\, \boldsymbol{B}_v\, F_v) dx
\end{aligned} \tag{4.7}$$

At this point is possible to transfer the integral only on x dependent terms and rewrite the governing equation in a arrayal form:

$$[\delta\hat{\boldsymbol{u}}, \delta\hat{\boldsymbol{v}}, \delta\hat{\boldsymbol{\sigma}}, \delta\hat{\boldsymbol{\tau}}] \begin{bmatrix} \mathbf{0} & \mathbf{0} & \boldsymbol{K_{u\sigma}} & \boldsymbol{K_{u\tau}} \\ \mathbf{0} & \mathbf{0} & \mathbf{0} & \boldsymbol{K_{v\tau}} \\ \boldsymbol{K_{\sigma u}} & \mathbf{0} & \boldsymbol{K_{\sigma\sigma}} & \mathbf{0} \\ \boldsymbol{K_{\tau u}} & \boldsymbol{K_{\tau v}} & \mathbf{0} & \boldsymbol{K_{\tau\tau}} \end{bmatrix} \begin{Bmatrix} \hat{\boldsymbol{u}} \\ \hat{\boldsymbol{v}} \\ \hat{\boldsymbol{\sigma}} \\ \hat{\boldsymbol{\tau}} \end{Bmatrix} = \begin{Bmatrix} \hat{\boldsymbol{F}}_u \\ \hat{\boldsymbol{F}}_v \\ \mathbf{0} \\ \mathbf{0} \end{Bmatrix} \tag{4.8}$$

The matrix $\boldsymbol{K}$ we have just introduced is usually called "*stiffness matrix*" and its terms are defined as follows:

$$\boldsymbol{K_{u\sigma}} = \int_l \boldsymbol{B}_u'^T \boldsymbol{P_{u\sigma}} \boldsymbol{B}_\sigma dx \qquad \boldsymbol{K_{v\tau}} = \int_l \boldsymbol{B}_v'^T \boldsymbol{P_{v\tau}} \boldsymbol{B}_\tau dx \tag{4.9a}$$
$$\boldsymbol{K_{u\tau}} = \int_l \boldsymbol{B}_u^T \boldsymbol{P_{u'\tau}} \boldsymbol{B}_\tau dx \qquad \boldsymbol{K_{\sigma u}} = \int_l \boldsymbol{B}_\sigma^T \boldsymbol{P_{\sigma u}} \boldsymbol{B}_u' dx \tag{4.9b}$$
$$\boldsymbol{K_{\tau v}} = \int_l \boldsymbol{B}_\tau^T \boldsymbol{P_{\tau v}} \boldsymbol{B}_v' dx \qquad \boldsymbol{K_{\tau u}} = \int_l \boldsymbol{B}_\tau^T \boldsymbol{P_{\tau u'}} \boldsymbol{B}_u dx \tag{4.9c}$$
$$\boldsymbol{K_{\sigma\sigma}} = \int_l \boldsymbol{B}_\sigma^T \boldsymbol{P_{\sigma\sigma}} \boldsymbol{B}_\sigma dx \qquad \boldsymbol{K_{hh}} = \int_l \boldsymbol{B}_\tau^T \boldsymbol{B_{\tau\tau}} \boldsymbol{P}_\tau dx \tag{4.9d}$$
$$\hat{\boldsymbol{F}}_i = \int_l \boldsymbol{B}_u^T \boldsymbol{F_u} dx \qquad \hat{\boldsymbol{F}}_j = \int_l \boldsymbol{B}_v^T \boldsymbol{F_v} dx \tag{4.9e}$$

4.3 Hypotheses

4.3.1 New base functions and numerical problem definitions

The choice of shape functions is a critical step in definition of FEM (Finite Element Method) algorithm: the accuracy and efficiency of the algorithm depends on it.

The multi-layered beam defined in chapter 2 uses a high number of unknowns (being n the number of layers, the unknown functions in the beam are $3n+2$ displacements and $6n-1$ stresses). Supposing the continuity of every unknown function to be necessary, we are going to define an enormous stiffness matrix, in other words a low-efficiency numerical algorithm. To remedy this problem we will make the following choice.

- We assume inter-element discontinuous functions to model stresses. Looking at the structure of $\boldsymbol{K}$ and using this hypothesis we can operate a static condensation on the element stiffness matrix, reducing the dimension of global algebraic problem and with the possibility to evaluate stress magnitude in post processing.

- We split displacement field as follows: $\boldsymbol{s} = \boldsymbol{s}_T + \boldsymbol{s}_W$ in which $\boldsymbol{s}_T$ are the Timoshenko displacements that use base functions globally defined on the section while $\boldsymbol{s}_W$ are the warping displacements and are locally defined on the layers as illustrated in figure 2.9. In the numerical model,

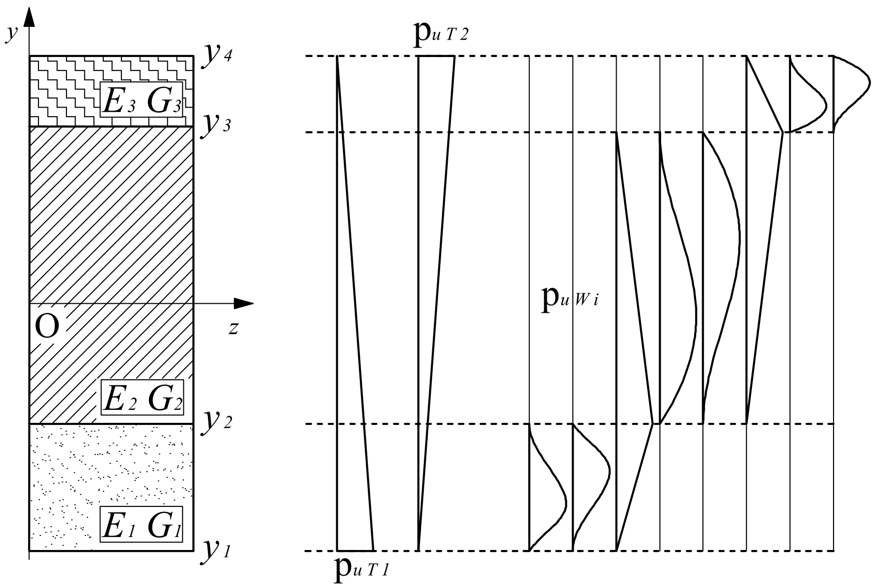

Figure 4.1: Section base functions used in FEM algorithm

as shape functions we will use continuous piecewise defined functions to model the Timoshenko displacements and bubble functions to the warping components. With this choice we simplify the assembling procedure and improve the stiffness matrix scatter-plot.

4.3.2 Shape function local definition

In the numerical algorithm we are going to use, for every unknown the following shape functions. $\tilde{x}$ is the element local coordinate and $\tilde{l}$ is the element length.

- Transversal displacement v is modeled by cubic shape functions defined as follows:

$$\boldsymbol{q}_v = \left\{ \begin{array}{c} 2\,\dfrac{\tilde{x}^3}{\tilde{l}^3} - 3\,\dfrac{\tilde{x}^2}{\tilde{l}^2} + 1 \\ \dfrac{\tilde{x}^3}{\tilde{l}^2} - 2\,\dfrac{\tilde{x}^2}{\tilde{l}} + \tilde{x} \\ -2\,\dfrac{\tilde{x}^3}{\tilde{l}^3} + 3\,\dfrac{\tilde{x}^2}{\tilde{l}^2} \\ \dfrac{\tilde{x}^3}{\tilde{l}^2} - \dfrac{\tilde{x}^2}{\tilde{l}} \end{array} \right\} \tag{4.10}$$

  In figure 2.18 we report the plot of shape function. By this shape function we obtain a solution $v(x) \in C^1$.

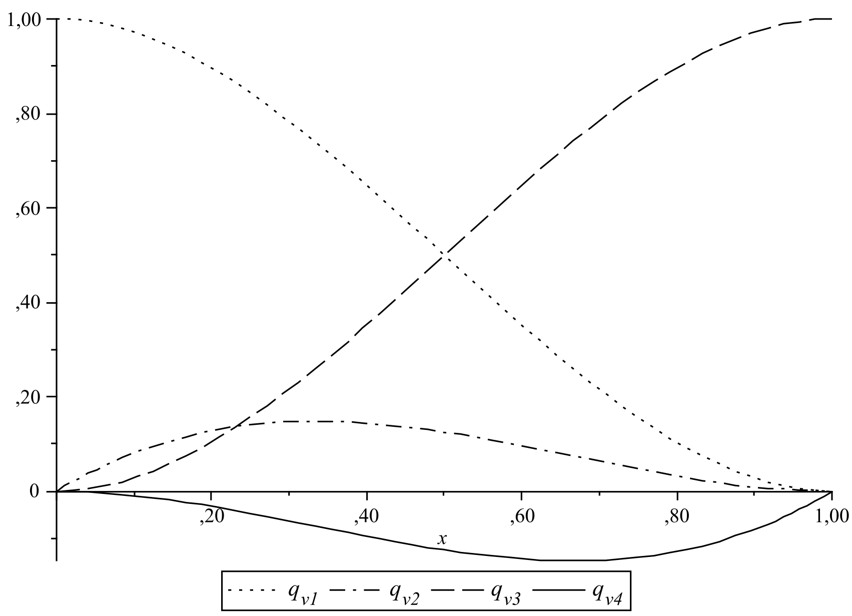

Figure 4.2: v shape functions

- Timoshenko horizontal displacements $\boldsymbol{u}_T$ are modeled by linear piecewise functions, defined as follows:

$$\boldsymbol{q}_{u_T} = \left\{ \begin{array}{c} \dfrac{\tilde{l} - \tilde{x}}{\tilde{l}} \\ \dfrac{\tilde{x}}{\tilde{l}} \end{array} \right\} \tag{4.11}$$

In this way we obtain a C^0 solution for these functions.

- Warping horizontal displacements $\boldsymbol{u}_W$ are modeled by a quadratic bobble, defined as follows:

$$q_{u_W} = 4 \frac{\left(\tilde{l} - \tilde{x}\right) \tilde{x}}{\tilde{l}^2} \tag{4.12}$$

In this way we obtain a C^0 solution for these functions that are null in the mesh nodes.

- Stresses are modeled by quadratic shape functions defined as the union of $\boldsymbol{q}_{u_T}$ and q_{u_W}.

4.4 Numerical examples

In the following we will discuss the results of the numerical algorithm we have just defined and we will report plots for some significant examples.

4.4.1 Bending moment loaded cantilever

We consider the laminated beam we have already presented in section 3.2. As unique load we consider an unitarian bending moment applied at one extremity while as boundary condition we clamp the other beam extremity. By the load characteristics we can deduce that the bending moment is constant inside the length of beam, so the shear is null and the rotation magnitude is linear. In these conditions the laminated, material homogeneous beam we are considering must give exactly the EB solution, moreover being the shape functions sufficiently rich, we expect that also the numerical model may catch the exact solution using only 1 element.
In figures 4.3 and 4.4 we plot the solution as obtained by the numerical model using 1 element. In table 4.1 we report numerical value of unknowns found with analitical and numerical models. It is possible to see how the numerical model catches exactly the solution.

4.4.2 Shear loaded cantilever

Now we are going to consider once again the laminated beam introduced in section 3.2 but, differently from what we did in previous section we will

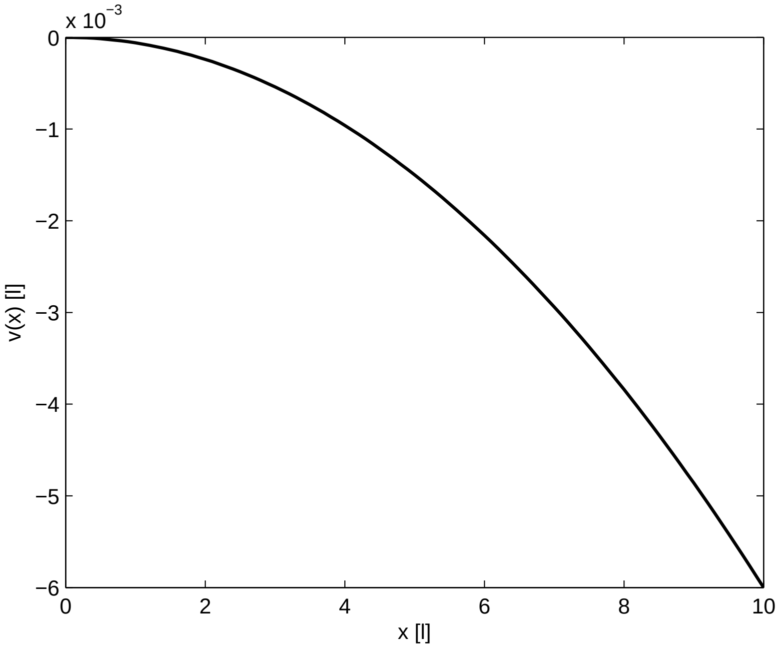

Figure 4.3: Transversal displacements of a cantilever loaded by extreme concentrated bending moment

quantities	num. mode	EB model
v(0)	0.0000	0.0000
v(l)	$-\ 6.0000 \times 10^{-3}$	$-\ 6.0000 \times 10^{-3}$
v'(0)	1.5710×10^{-42}	0.0000
v'(l)	1.2000×10^{-3}	1.2000×10^{-3}
$\vartheta(l)$	$-\ 1.2000 \times 10^{-3}$	$-\ 1.2000 \times 10^{-3}$

Table 4.1: Displacements at significant sections

consider a transversal load in the extremitiy of the beam.
In the analytical solution the rotations are parabolic, on the opposite the numerical model contains only linear horizontal displacements so we expect an error in the numerical solution. To improve the solution we must use more elements. In figures 4.5, 4.6 and 4.7 we report the solutions as obtained by the TJ analytical model and by the numerical model, in the latter considering 1, 2 and 4 elements. In figures 4.8 and 4.9 we plot the magnitudes of an axial stress component (σ_1) and of a shear stress component (τ_3) for 2, 4 and 8 elements.

It is possible to see how the solution error becomes quickly small increasing the number of elements, moreover we can observe how the rotations are exactly evaluated at nodes. It is possible to see also an error on the free

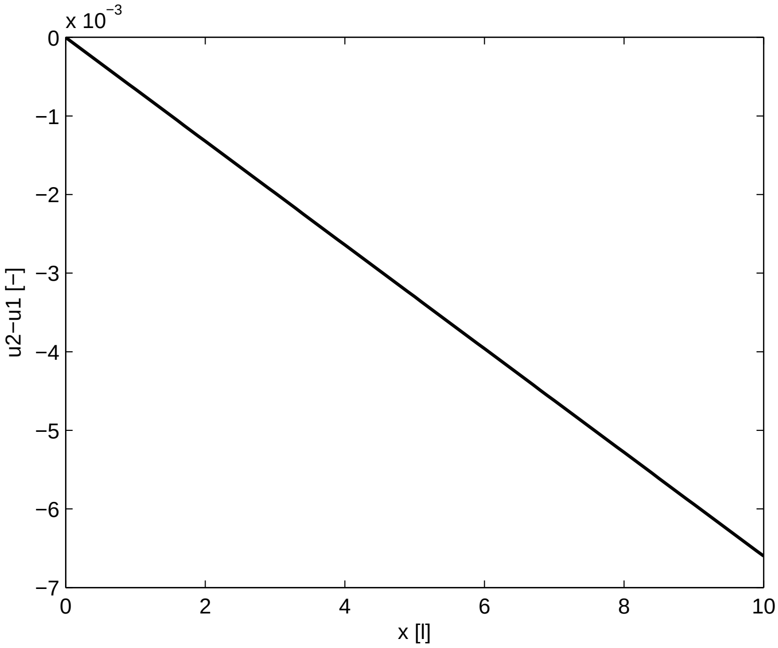

Figure 4.4: Section rotations of a cantilever loaded by extreme concentrated bending moment

extreme displacements: in table 4.2 we write the magnitude of these errors as function of the number of elements used. Looking at the table we can say that the solution displays a good convergence to the exact solution, moreover we can see that the relative error is near the 1 % also using few elements. In figure 2.25 we plot the section shear distribution on the node $x = 5,000$ and at the half of element 4 ($x = 4.375$) as calculated using 8 elements. It is clear that inside the element the model predicts exactly the shear distribution while in the nodes, being null the warping, shear distribution tends to become constant and, in any case far from the exact solution.

elem n	v(l)	$\frac{v(l)}{v_{TJ}(l)}$
1 el	-3.92×10^{-2}	0.9727
2 el	-3.99×10^{-2}	0.9901
4 el	-4.02×10^{-2}	0.9975
8 el	-4.027×10^{-2}	0.9993
TJ model	-4.03×10^{-2}	1.0000

Table 4.2: Free extreme transversal displacement

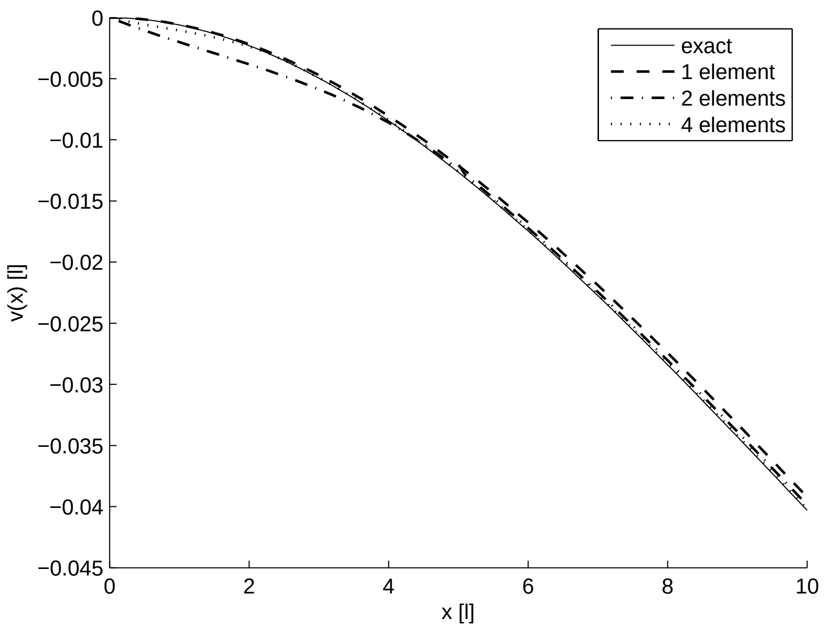

Figure 4.5: Transversal displacements of a cantilever loaded by extreme shear resultant

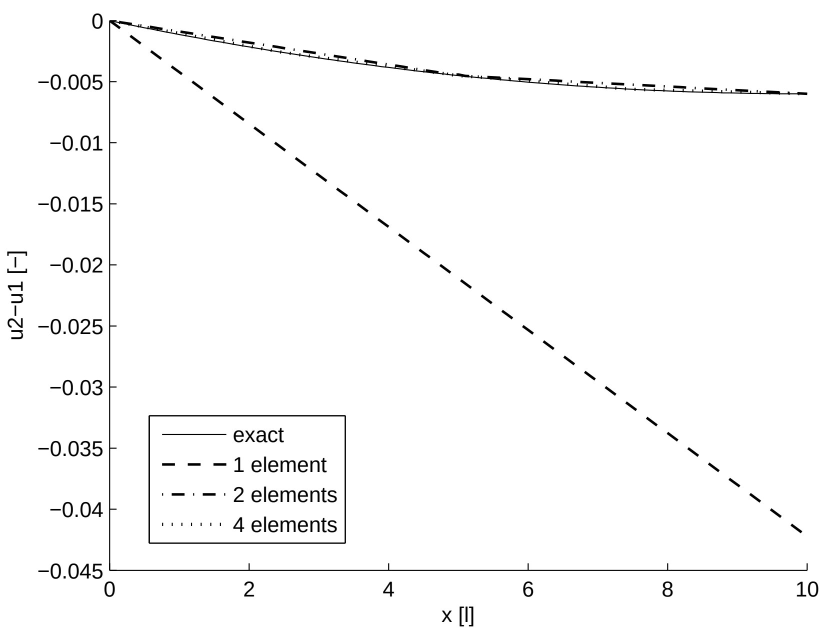

Figure 4.6: Section rotations of a cantilever loaded by extreme shear resultant

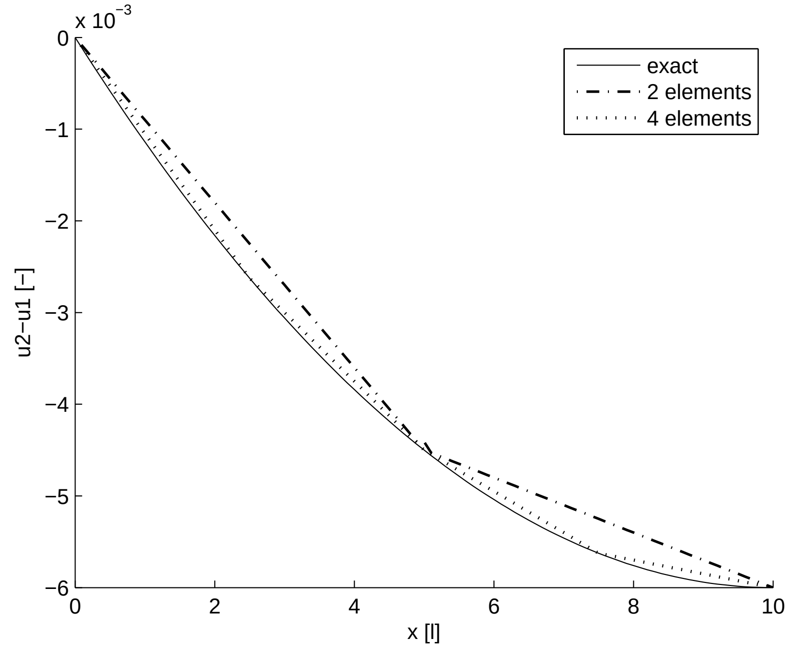

Figure 4.7: Section rotations of a cantilever loaded by extreme shear resultant (detail)

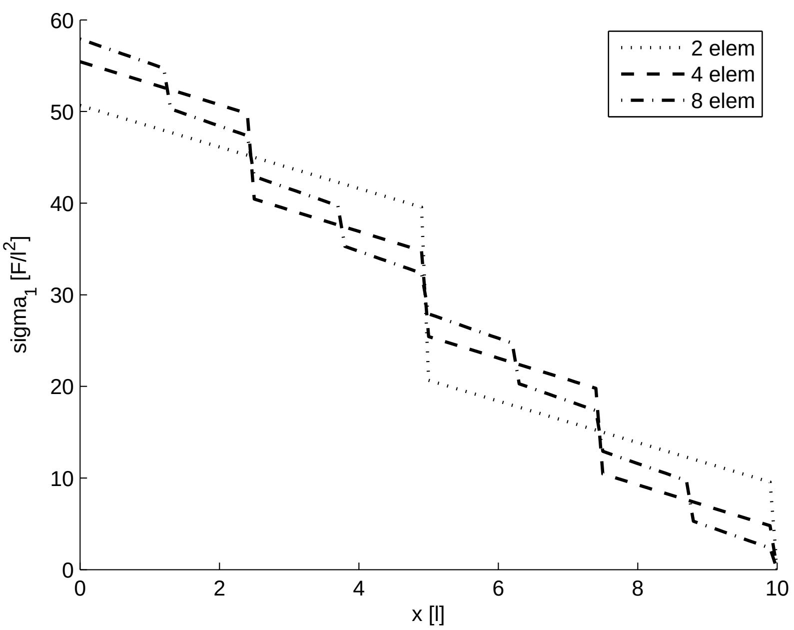

Figure 4.8: Axial stress component σ_1 of a cantilever loaded by extreme shear resultant

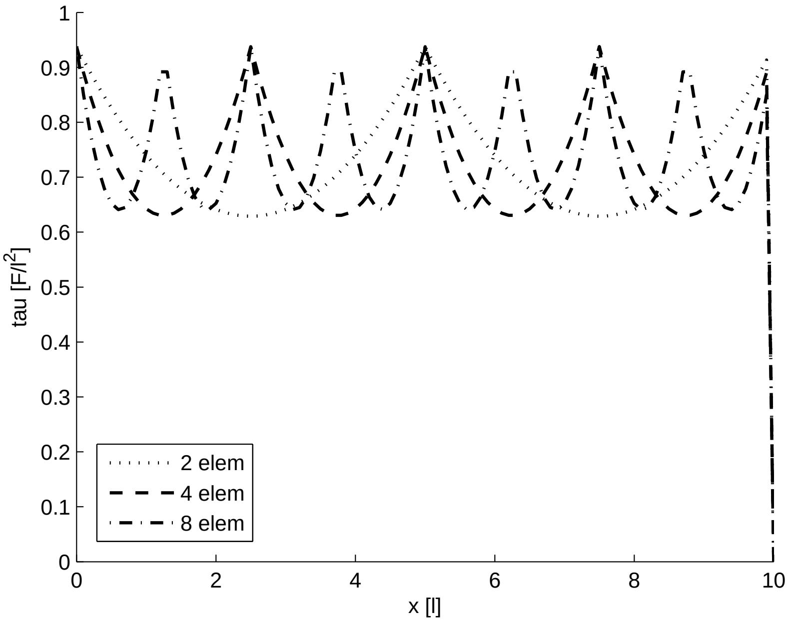

Figure 4.9: Shear stress component τ_3 of a cantilever loaded by extreme shear resultant

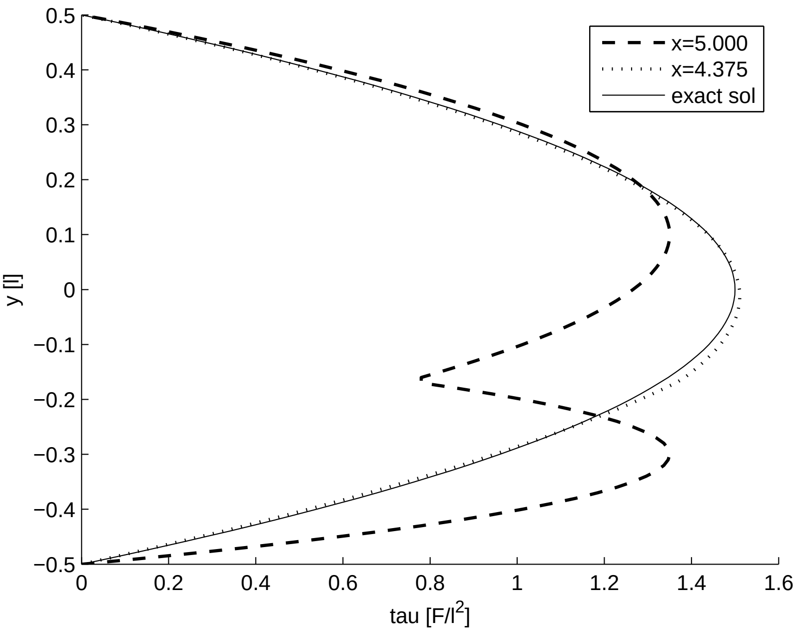

Figure 4.10: Section shear distribution on the nodes ($x = 5.00$) and at the half of the element length ($x = 4.375$)

Chapter 5

Conclusions

In this thesis we discussed some models of homogeneous and laminated beams, for the latter we developed also a FEM model.

The analytical models can predict in a correct way the internal stress distribution and do not need to be corrected by any factor, as happens in Timoshenko beam. Moreover, looking at laminated beam, the model we developed can predict the answer of the body to local effects.

As far as the numerical model is concerned, we wrote an algorithm that uses a low number of degrees of freedom, in particular stresses are locally static condensated and the global stiffness matrix is formulated as a function of nodal linear displacements and some bubbles that account the high order section displacements. In post processing it is possible to evaluate stresses that estimate correctly the real ones.

A possible development of this work might be the improvement of the FEM model to enhance the prediction of stress distributions, and model generalization to non-planar stress and kinematics.

Bibliography

[1] S. M. Alessandrini, D. N. Arnold, R. S. Falk, A. L. Madureira *Derivation and justification of plate models by variational methods*, CRM Proceedings and Lecture Notes, 21, Amer. Math. Soc. (1999), pp. 1-20.

[2] F. Auricchio, E. Sacco, *A mixed FSDT finite-element for the analysis of laminated plate with no shear-correction factor*, (2002).

[3] J.M. Bairan, A.R. Mari, *Coupled model for the non-linear analysis of anisotropic sections subjected to general 3D loading. Part 1: Theoretical formulation*, Computers and Structures 84 (2006), 2254-2263.

[4] J.M. Bairan, A.R. Mari, *Coupled model for the non-linear analysis of anisotropic sections subjected to general 3D loading. Part 2: Implementation and validation*, Computers and Structures 84 (2006), 2264-2276.

[5] J.M. Bairan, *Doctoral thesis: "A non-linear coupled model for the analysis of reinforced concrete sections under bending, shear, torsion and axial forces"*, Barcelona 2005 chapters 2-3.

[6] V. Franciosi, *Fondamenti di scienza delle costruzioni, volume secondo "Teoria della trave"*, Liguori editore (1978).

[7] L. Corradi Dell'Acqua *Meccanica delle strutture, volume primo, "Il comportamento dei mezzi continui"*, McGraw - Hill (1992).

[8] L. Corradi Dell'Acqua *Meccanica delle strutture, volume secondo, "Le teorie strutturali e il metodo degli elementi finiti"*, McGraw - Hill (1992).

[9] M.D. Hayes, *Doctoral thesis: "Structural analysis of a pultruded composite beam: shear stiffness determination and strength and fatigue life predictions" - Appendix A Third Order Laminated Beam Theory*, http://scholar.lib.vt.edu/ (2003).

[10] K.D. Hjelmstad, E. Taciroglu, *Variational basis of nonlinear flexibility methods for structural analysis of frames*, Journal of engineering mechanics (November 2005), 1157-1169.

[11] N.J. Pagano, *Exact solutions for rectangular bidirectional composites and sandwich plates*, Journal of composite materials 4 (january 1970), 20-34.

[12] N.J. Pagano, *Exact solutions for composite laminates in cylindrical bending*, Journal of composite materials 3 (july 1969), 398-411.

[13] R.L. Taylor *FEAP - A Finite Element Analysis Program - Theory manual*, University of California at Berkeley (January 2008).

[14] I. Sheinman *On the analytical colsed-form solution of high-order kinematic models in laminated beam theory*, Int. J. Numer. Meth. Engng. 50 (2001) 919-936.

[15] M. Tahani *Analysis of laminated composite beams using layerwise displacement theories*, Composite Structures 79 (2007) 535-547.

[16] I. Sheinman, M. Eisenberger, Y. Bernstein *High-order element for prebuckling and buckling analysis of laminated plane frames*, Int. J. Numer. Meth. Engng. 39 (1996) 2155-2168.

[17] P. Ladevèze, J. Simmonds, *New concepts for linear beam theory with arbitrary geometry and loading*, European Journal of Mechanics a/solids 17 (1998), 377-402.